NASA
Technical
Paper
2328

July 1984

NASA-TP-2328 19840019607

Recent Modifications and Calibration of the Langley Low-Turbulence Pressure Tunnel

Robert J. McGhee,
William D. Beasley,
and Jean M. Foster

NASA

NASA
Technical
Paper
2328

1984

Recent Modifications and Calibration of the Langley Low-Turbulence Pressure Tunnel

Robert J. McGhee,
William D. Beasley,
and Jean M. Foster

Langley Research Center
Hampton, Virginia

NASA
National Aeronautics
and Space Administration

**Scientific and Technical
Information Branch**

ABSTRACT

A description is presented of recent modifications to the Langley Low-Turbulence Pressure Tunnel, and a calibration of the mean flow parameters in the test section is provided. Also included are the operational capability of the tunnel and typical test results for both single-element and multi-element airfoils.

Modifications to the facility consisted of the following: replacement of the original cooling coils and antiturbulence screens and addition of a tunnel-shell heating system, a two-dimensional model-support and force-balance system, a sidewall boundary-layer control system, a remote-controlled survey apparatus, and a new data-acquisition system.

A calibration of the mean flow parameters in the test section was conducted over the complete operational range of the tunnel. The calibration included dynamic-pressure measurements, Mach number distributions, flow-angularity measurements, boundary-layer characteristics, and total-pressure profiles. In addition, test-section turbulence measurements made after the tunnel modifications have been included with these calibration data to show a comparison of existing turbulence levels with data obtained for the facility in 1941 with the original screen installation.

INTRODUCTION

The Langley two-dimensional Low-Turbulence Pressure Tunnel (LTPT) began operation in about 1941. A description and history of the tunnel are provided in reference 1. The tunnel was designed for testing airfoil sections at high Reynolds numbers approaching full-scale values and for extremely low airstream turbulence levels for laminar-flow airfoil research. High Reynolds numbers were obtained by increasing the tunnel air density up to 10 atm (147 psia), and low turbulence was obtained by using a large contraction ratio and a number of fine-wire small-mesh screens in the settling chamber.

The tunnel also has a sting- and strut-mount model-support system for testing small-span three-dimensional models. Force and moment data are measured with internal strain-gage balances.

For the past several years, the Langley Research Center has initiated research programs in the areas of viscous drag reduction and high-Reynolds-number aerodynamics. The Langley Low-Turbulence Pressure Tunnel is well suited for research in both of these areas at low subsonic Mach numbers. As the tunnel was approximately 40 years old, rehabilitation of the tunnel was undertaken. The two main objectives of the rehabilitation were to restore and improve the flow quality required for future laminar-flow research and to provide a two-dimensional model-support and force-balance system for high-Reynolds-number testing of both single-element and multi-element airfoils.

Improvements to the tunnel which were accomplished during the rehabilitation were replacement of the original cooling coils and antiturbulence screens and

addition of a tunnel-shell heating system, a two-dimensional model-support and force-balance system, a sidewall boundary-layer control system, a remote-controlled survey apparatus, and a new data-acquisition system.

This report describes the wind-tunnel modifications, the complete calibration of the tunnel, and the operational capability of the tunnel. Also included are typical results for both single-element and multi-element airfoils.

SYMBOLS

CF tunnel calibration factor, $\dfrac{p_{t,p} - p_p}{p_{t,ref} - p_{ref}}$, with p_p averaged from $x = -20$ in. to $x = 20$ in.

C_p pressure coefficient, $\dfrac{p_\ell - p_\infty}{q_\infty}$

c airfoil chord, in.

c_d section profile-drag coefficient, $\int_{Wake} c'_d \, d\left(\dfrac{h}{c}\right)$

c'_d point-drag coefficient,

$$2\left(\frac{p}{p_\infty}\right)^{6/7}\left[\frac{(p_t/p)^{2/7} - 1}{(p_{t,\infty}/p_\infty)^{2/7} - 1}\right]^{1/2}\left\{\left(\frac{p_t}{p_{t,\infty}}\right)^{1/7} - \left[\frac{(p_t/p_\infty)^{2/7} - 1}{(p_{t,\infty}/p_\infty)^{2/7} - 1}\right]^{1/2}\right\}$$

c_l section lift coefficient

c_m section pitching-moment coefficient about quarter-chord point

h vertical distance in wake profile, in.

M free-stream Mach number

M_ℓ local Mach number

M_p probe Mach number

$\dot{m}_b$ blowing-box mass-flow rate, slugs/sec

$\dot{m}_{ts}$ test-section mass-flow rate, slugs/sec

p static pressure, psf

p_p probe static pressure (free-stream), psf

p_{ref} tunnel sidewall reference static pressure, psf

p_t total pressure, psf

$p_{t,p}$ probe total pressure (free-stream), psf

$p_{t,ref}$ tunnel reference total pressure, psf

q dynamic pressure, psf

R unit Reynolds number

R_c Reynolds number based on airfoil chord

u_∞ free-stream velocity

u/u_∞ ratio of local boundary-layer velocity to free-stream velocity

u_s/u_∞ ratio of slot-exit velocity to free-stream velocity

X,Y,Z axes of tunnel coordinate system (fig. 16)

x,y,z local dimensions in tunnel coordinate system, in. (x also denotes airfoil abscissa in fig. 41)

α angle of attack, deg

δ aerodynamic instrument error for yawmeter, deg

ε flow angle measured in vertical plane (positive up), deg

Subscripts:

ℓ local conditions

ref reference

∞ free-stream conditions

1 reference static pressure orifice at x = -38 in.

2 reference static pressure orifice at x = -64.5 in.

Abbreviations:

AOA angle of attack

BLC boundary-layer control

Dia. diameter

LTPT Langley Low-Turbulence Pressure Tunnel

Rad. radius

WIND TUNNEL AND MODIFICATIONS

General Description

The Langley Low-Turbulence Pressure Tunnel (described in detail in ref. 1) is a single-return, closed-throat tunnel which can be operated at pressures from near-vacuum to 10 atmospheres. An exterior view of the tunnel is shown in figure 1, and a sketch of the tunnel circuit arrangement is shown in figure 2. The test section is rectangular in shape, 3 ft wide, 7.5 ft high, and 7.5 ft long. The contraction ratio is 17.6:1. The test-section sidewalls have an outward total divergence of about 0.0038 in/in. (from tunnel stations -20 in. to 40 in.) to allow for the growth of the boundary layer on the sidewalls.

A 350-psi offsite air supply system provides dry compressed air to the facility. Onsite storage tanks are utilized with an air capacity of 8000 ft^3 at 300 psi. A centrifugal five-stage compressor with a volume flow of about 15 000 ft^3/min powered by a 5500-horsepower drive motor supplies the air. The air is dried by an activated-alumina dryer system with a volume flow of 14 000 ft^3/min. Air-outlet dewpoint temperature of about -30°F is generally maintained. An onsite compressor with a volume flow of 2400 ft^3/min is used as an exhauster for tunnel vacuum operation. The tunnel also serves as an air storage vessel for operation of the Langley 6- by 28-Inch Transonic Tunnel.

Modifications

Heat exchanger.- Since the tunnel operates at pressures up to 10 atm and because of the age of the structure, the tunnel shell was subjected to nondestructive examinations, and necessary repairs were made in 1974 to extend the useful life of the tunnel. The tunnel was recertified for operation at pressures up to 10 atm subject to the pressure-temperature restriction shown in figure 3. This pressure-temperature restriction limited the tunnel pressure to 5 atm for cold weather conditions (below 20°F). Thus, the deteriorated cooling coils were replaced with a heat exchanger to provide both heating and cooling of the airstream. The heating mode is used in extremely cold weather operation to permit tunnel pressures up to 10 atm. The heat exchanger has an automatic temperature system that utilizes three steam injectors with modulated valves to control both temperature and volume flow of water through the coils (fig. 4). The energy expended by the main-drive system is removed by the water flowing through the coils and transmitted to the atmosphere through a cooling tower located outside the facility.

Tunnel shell heaters.- To further improve tunnel operation during extremely cold weather, preheating of the tunnel shell in areas inaccessible to the heated airstream was provided. Electric space heaters were installed in the test chamber of the tunnel, and strip heaters were added on the outside shell of the test chamber (fig. 5). The strip heaters were covered with fiberglass insulation and enclosed with a metal cover. Other regions of the outside tunnel shell were covered with a 2-in-thick coat of urethane foam under an exterior vinyl coating.

Screen installation.- Over the past four decades, a number of the original antiturbulence screens were removed, and the remaining seven screens had become contaminated with oil and debris. For these reasons, new screens were selected and installed. An analysis of the screen parameters was conducted by Dan M. Somers of the Langley Research Center.

The objective of the new screen design was to increase the critical Reynolds number of the screens and, thereby, increase the maximum Reynolds number for which low turbulence could be maintained. This objective was accomplished by reducing the wire diameter of the screens from 0.0065 in. to 0.0050 in. A single constraint was placed on the new screen design to allow the existing attachment hardware to be used. The load on each new screen, and hence the pressure drop across each screen, had to be equal to or less than that of the original screen. Thus, the original screen solidity (35.2 percent) was retained. This was achieved by increasing the mesh from 30 to 39. The wire material was also changed from phosphor bronze to stainless steel to accommodate the higher stress in the smaller diameter wire.

Nine identical screens were installed, and the original 3-in. spacing between each screen was retained. The photograph in figure 6 shows a single screen installation (looking upstream). Because of advances in manufacturing techniques, each new screen was produced in a seamless 21-ft by 21-ft piece, as opposed to the 7-ft-wide strips which were hand-sewn together to make the original screens.

Model-support and force-balance system.- A major part of the tunnel renovation was the installation of a new model-support and force-balance system capable of handling both single-element and multi-element airfoils for high-Reynolds-number testing. This new support system is shown in figures 7 and 8. The airfoil model is mounted between two end plates, which are connected to the inner drums. The inner drums are held in place by an outer drum and yoke-arm support system. The yoke support system is mounted to the balance, which is, in turn, connected to the tunnel through a balance platform. The yoke arm is fabricated from aluminum in a monocoque structure to minimize weight loads on the balance system. The attitude of the model is controlled by a motor-driven, externally mounted pitch mechanism that rotates the bearing-mounted inner drums. A multipath labyrinth seal (see fig. 7) is used to minimize air leakage from the test section into the outer tunnel plenum. An electrical fouling indicator is incorporated in the seal to detect any fouling at the seal components.

The new three-component strain-gage balance is of the external virtual-image type. The balance design loads are 18 000 lb in lift, 550 lb in drag, and 12 000 ft-lb in pitching moment. The balance is temperature compensated and calibrated to account for first- and second-order interactions such that the system is generally accurate to within ± 0.5 percent of the design loads. The balance was calibrated onsite in the tunnel. A photograph of the balance is shown in figure 9.

Sidewall boundary-layer control system.- To insure two-dimensionality of the flow field when testing multi-element airfoils, some form of tunnel sidewall boundary-layer control (BLC) is needed. The large adverse pressure gradients induced by the high-lift airfoil can cause the tunnel sidewall boundary layer to separate and result in a decrease in airfoil lift. Since a source of high-pressure air was available for the tunnel, tangential blowing was selected to provide sidewall BLC. Five blowing boxes with tangential slots are available for each side of the tunnel and can be positioned around the airfoil within the confines of the end plates. High-pressure air is supplied to each box through a flexible hose connected to a mobile blowing-box control cart. (See fig. 10.) Low-friction swivel connectors are provided at each end of the flexible hose to allow rotation of the model and also to minimize the effects of the hoses on the balance measurements. The control carts also contain flowmeters to monitor the amount of air injected thru the blowing-box slots into the tunnel. An automatic control valve is utilized to remove the air injected into the tunnel by the BLC system and to maintain a constant total pressure in the tunnel.

A schematic representation of the BLC system is shown in figure 11. Compressed dry air is provided from a 4-in-diameter supply pipe to each side of the tunnel test section. Flow rates are monitored and controlled automatically to maintain constant flow rates to the control carts. A distribution manifold mounted on the cart feeds a dual flow loop to provide air to the individual blowing boxes. Flow rates are controlled in each loop by valves to provide the desired flow rates to the blowing boxes. The operating pressure for the BLC system is 300 psi, and the maximum total flow rate is about 35 lb/sec.

The blowing boxes were designed to provide uniform tangential flow at the slot exit. (See fig. 12.) Air enters an inner manifold distribution chamber and is distributed through slots to an outer manifold chamber. The exit slot is formed by a removable slot lip and the box itself. The width of the slot exit may be varied by utilizing different slot lips.

Remote-controlled survey apparatus.- The survey apparatus is shown schematically in figure 13, and a photograph of the apparatus mounted in the wind tunnel is shown in figure 14. The apparatus basically consists of an articulating arm mounted on an arc strut. Movement of the arm enables surveys using probes (pressure, flow angularity, hot-wire) to be made over a range of positions in the tunnel test section.

The arm is composed of three movable components: a main boom, an offset boom, and a forward-pivoting head. Each component has a position control device. The main boom is mounted on the strut with a pivot point allowing rotation in the vertical plane. Its motion is controlled by the linear actuator. The offset boom can be rotated about the main boom by the roll actuator. This allows survey positions to be made at distances up to 12 in. from the tunnel centerline. The forward-pivoting head is mounted at the end of the offset boom and may be rotated in the vertical plane by the (internally mounted) pitch adjustment mechanism. Figure 13 shows the survey apparatus with a wake rake mounted on the forward-pivoting-head assembly. In addition, the entire apparatus can be positioned vertically in the wind tunnel by utilizing the movable strut, which moves within the confines of fixed leading- and trailing-edge fairings. The position and rate of movement of any survey device mounted on the apparatus are controlled by a microprocessor controller. Wake rake surveys using the remote-controlled apparatus (to obtain the profile drag of an airfoil) provided acceptable drag results with a survey rate of about 0.10 in/sec.

Data-acquisition system.- The heart of the on-line data-acquisition system is a computer with a random access memory of 512K bytes (fig. 15) coupled to a data-acquisition system with 192 analog and 16 digital recording channels. This system provides on-line data reduction and displays in real time, as well as instrumentation calibration capability for the Low-Turbulence Pressure Tunnel. Force and moment data are measured with strain-gage balances which are temperature compensated and calibrated to account for first- and second-order interactions such that the system is generally accurate to within ± 0.5 percent of the design balance loads. Pressure data are taken with variable-capacitance precision transducers used with scanning valves. The data-acquisition system can accommodate up to ten 48-port scanning valves. The pressure transducers are automatically calibrated and are accurate within ± 0.5 percent of the reading plus 0.005 percent of the transducer rating. Each data point is generally computed on-line from 10 scans of data taken over a 1-sec interval. Traversing probe data are taken in a continuous mode, and the number of samples changes with survey length and distance set between points instead of time intervals. Real-time data plots are displayed on cathode-ray tubes, and the system has hard-copy

capability. Tunnel parameters are computed in engineering units and displayed in real time on a color cathode-ray tube.

CALIBRATION AND TUNNEL OPERATING CHARACTERISTICS

Calibration

Procedure.- The Langley Low-Turbulence Pressure Tunnel has been calibrated to determine mean flow parameters in the test section. The general calibration arrangement (fig. 16) consisted of a long survey probe aligned with the longitudinal centerline of the test section. The nose of the probe contained a total-pressure tube, and static-pressure orifices were installed flush with the probe surface at fixed interval distances over the probe length. These were used to measure the probe total-pressure and static-pressure distribution of the airstream. Also shown in figure 16 are the reference total-pressure probes on the floor of the wind tunnel and the tunnel sidewall reference static-pressure orifices from which the tunnel test conditions are calculated. A photograph of the probe mounted in the tunnel is shown in figure 17.

A tunnel calibration factor which relates the probe total pressure and average probe static pressures over the test section (averaged from $x = -20$ in. to $x = 20$ in.) to the tunnel reference total pressure and sidewall reference static pressures was determined for the entire operational boundaries of the facility. The effect of tangential blowing of high-pressure air through several slots in the tunnel test section (sidewall boundary-layer control system for airfoil tests) on the basic tunnel calibration factors was also determined. Other test-section flow parameters that were measured during the calibration were turbulence levels, dynamic-pressure variations, flow angularity, total-pressure profiles, and sidewall boundary-layer profiles. Details of the various probes used to measure the test-section flow parameters are shown in figure 18.

Tunnel calibration factors.- Figure 19 shows the tunnel calibration factor (CF) (the ratio of the differences between the probe total and static pressures and the reference total and static pressures) as a function of Mach number for the tunnel operational range. Two calibration factors based on sidewall static orifices located at tunnel stations of -38 in. ($p_{ref,1}$) and -64.5 in. ($p_{ref,2}$) are shown. Four sidewall (two on each sidewall) static orifices located 15 in. above and below the tunnel centerline were teed together and used as the reference pressure at tunnel station $x = -38$ in. Two sets of static orifices located 1.5 in. above and below the tunnel centerline were provided at tunnel station $x = -64.5$ in. One set was used as the reference pressure, and the other set served as a backup. The CF based on the static orifices at station -38 in. (normally used for single-element airfoil tests) is shown to vary less than 0.25 percent over the entire Mach number and Reynolds number ranges of the tunnel (fig. 19). The CF based on the static orifices at station -64.5 in. (used for high-lift testing to minimize model effects on reference static pressure) is a function of Mach number, as expected, because the reference static orifice is located in the tunnel contraction region.

The effects of tangential blowing of high-pressure air through several sidewall slots located in the test section (see fig. 16) on the basic tunnel calibration factors are illustrated in figure 20. Sidewall blowing is used for tunnel sidewall boundary-layer control for high-lift airfoil testing. Blowing decreases the tunnel CF at both stations; however, a larger decrease occurs for the CF based on the sidewall static pressures located at station -38 in. Note, however, that the effect of

blowing on the tunnel CF is less than 1 percent for blowing mass-flow rates as large as 0.40 percent of the tunnel test-section mass flow.

Mach number distributions.- Typical Mach number distributions calculated from floor and ceiling static pressures, survey probe static pressures, and probe total pressure are illustrated in figure 21. The data show that the flow is uniform between tunnel stations of about -40 in. to 40 in. Maximum variations in local Mach number are about ±0.002 for Mach numbers less than about 0.22 and about ±0.004 for Mach numbers greater than about 0.22. However, in the test region normally occupied by an airfoil model (x = -20 in. to 20 in.), the maximum variation in Mach number is about ±0.50 percent. The effect of sidewall blowing on the centerline Mach number distribution is shown in figure 21(c). The maximum variation in Mach number within the test region was about 2 percent for blowing mass-flow rates of about 0.40 percent of the tunnel mass flow (slot flow choked).

Dynamic-pressure (q) variations.- Dynamic-pressure surveys were made in the tunnel test section by using vertical and horizontal rakes of standard pitot-static probes designed according to reference 2 (pp. 91-95). The probes were 0.1875 in. in diameter, and in order to minimize tip and stem interference effects on static pressure, the orifices were located 8 probe diameters from the probe tip and 42 probe diameters from the probe mount. Details of the probe arrangement are shown in figures 18(a) and 18(b), and photographs of the probes mounted in the tunnel are shown in figures 22 and 23. The vertical rake was mounted alternately between the ceiling or floor and the centerline survey probe, and the horizontal rake was mounted alternately between the east or west sidewall and the survey probe. (See fig. 18(a).) In addition, a horizontal rake (figs. 18(b) and 23) was mounted between the east and west sidewalls with the centerline survey probe removed to eliminate any possible interference of the survey probe on the static pressure of the pitot-static probe.

Typical cross-sectional dynamic-pressure variations in the tunnel test section are illustrated in figure 24. The maximum deviation in dynamic pressure from the tunnel reference dynamic pressure was about 0.8 percent and occurred in a small core region near the center of the test section.

Test-section turbulence measurements.- Test-section turbulence was measured with a hot-wire anemometer by P. Calvin Stainback of the Langley Research Center after the installation of the new screens. As shown in figure 25, the present turbulence levels are about the same as for the original screens up to unit Reynolds numbers per foot of about 5×10^6. At the higher unit Reynolds numbers, some improvement in turbulence level was measured for the new screen installation.

Flow angularity.- The inclination of flow with respect to the tunnel centerline in the vertical plane was measured with claw-type yawmeters. The yawmeters were mounted on a wake survey rake used to make surveys behind an airfoil (fig. 18(c)). The yawmeters were positioned at various tunnel stations by using the remote-controlled survey apparatus. The yawmeter (fig. 18(c)) consists of two open-ended pressure probes facing upstream and inclined 90° with respect to each other. The yawmeters were calibrated in the tunnel by rotating the claw probe at various angles in both normal and inverted positions at various tunnel operating conditions. A typical calibration is shown in figure 26. The sensitivity of the yawmeter is expressed as the pressure difference between the two sensing holes per degree of pitch in terms of the stream dynamic pressure. Also indicated is the claw-probe aerodynamic instrument error δ.

Typical results of the flow angularity in the tunnel test section are shown in figure 27. Both positive and negative values of flow angle were measured; however, the maximum flow angle determined was less than 0.20°.

Total-pressure profiles.- Total-pressure surveys were made in the tunnel test section with the wake survey rake shown in figure 18(c). The rake was positioned at various tunnel stations by using the remote-controlled survey apparatus. The rake contained seven 0.063-in-diameter total-pressure tubes, which were flattened to an internal height of 0.02 in. over a length of 0.25 in. from the tip of the tube. Typical results of the surveys are illustrated by the map in figure 28. The results are shown as a percent deficit in total pressure ($p_t - p_{t,ref}$) in terms of the stream dynamic pressure. The data indicate that a total-pressure flow deficit is present in the middle of the test section. The maximum value of the deficit is about 0.8 percent of the stream dynamic pressure. A possible explanation for this total-pressure deficit is flow separation on the afterbody of the fan nacelle in the return leg of the tunnel. (See fig. 2.)

Test-section boundary layer.- Boundary-layer profiles have been measured on the tunnel test-section sidewalls both with and without sidewall boundary-layer control (tangential blowing). The measurements were obtained by using a rake (fig. 18(d)) of 15 tubes (0.062-in. outside diameter) spanning a distance of 3 in. perpendicular to the sidewall. The rake was mounted downstream of a typical blowing slot, as shown by the photograph in figure 17. Sidewall boundary-layer thickness with no tangential blowing varied from about 1.50 in. at $R = 1.5 \times 10^6$ per foot to about 1.2 in. at $R = 12.0 \times 10^6$ per foot at a Mach number of 0.22. Typical boundary-layer profiles with and without blowing are shown in figure 29. The velocities were calculated by assuming the static pressure across the boundary layer to be constant and equal to the free-stream static pressure. Tangential wall blowing energizes the sidewall boundary layer, and the velocity near the sidewall was increased from about $0.6u_\infty$ to about $1.3u_\infty$ for a slot mass-flow rate of about 0.004 slug/sec. Calculation of the sidewall boundary-layer displacement thickness for these two profiles indicated a value of about 0.18 in. for no blowing ($\dot{m}_b = 0$) compared with approximately zero with blowing ($\dot{m}_b = 0.004$).

Calibration of wake-rake static-pressure probes.- The drag of airfoils tested in the Low-Turbulence Pressure Tunnel is determined by the momentum method (ref. 2) by using a wake survey rake. The details of the rake are shown in figure 18(c), and a photograph of the rake is shown in figure 30. The remote-controlled survey apparatus is used for traversing the rake through the airfoil wake. The rake is composed of flow-angularity probes, total-pressure probes, and static-pressure probes. Two types of static-pressure probes were used, the standard type and the disc type. The standard-type probe consisted of a 0.125-in-diameter tube with a hemispherical head. Each static-pressure tube had eight flush orifices drilled 45° apart and located eight tube diameters from the tip of the tube. To obtain insensitivity to flow direction, a disc-type static probe was designed according to the technique described in reference 3. The disc probe was 0.437 in. in diameter and had a 0.018-in-diameter hole drilled through the center with an internal passage connecting this hole to the edge of the disc. (See fig. 18(c).)

Calibration of both static probes was performed to determine rake body effects, Mach number effects, and Reynolds number effects. The performances of the standard and disc static-pressure probes are shown in figures 31 and 32, respectively. The standard static-pressure probe was generally insensitive to Mach number ($M \leq 0.30$) and Reynolds number ($R \geq 1.5 \times 10^6$ per foot). The static-pressure reading was high by 8.20 percent of the stream dynamic pressure because of the rake body interference.

The variation of static pressure reading with flow inclination in pitch indicates that the calibration was valid up to a probe angle of about ±2°. The disc static probe was insensitive to Mach number ($M \leq 0.30$) and to flow inclination in pitch (±8°); however, large Reynolds number effects were measured. For example, for $R < 3.0 \times 10^6$ per foot, the static pressure reading was as much as 15 percent higher or lower than the stream dynamic pressure, depending on the value of Reynolds number. For $R \geq 3.0 \times 10^6$ per foot, the static pressure reading was within ±2 percent of the stream dynamic pressure.

Tunnel Operating Characteristics

The current operating range of test-section Mach number, unit Reynolds number, and dynamic pressure for the Low-Turbulence Pressure Tunnel is presented in figure 33. The tunnel operating regions shown represent constant temperature operations at 80°F. For any specific Mach number, the upper limit of unit Reynolds number is generally established by drive power and stagnation-pressure limits. A unit Reynolds number per foot as low as 100 000 can be obtained by operating the tunnel at vacuum conditions. However, for vacuum operations, special pressure instrumentation is required because of the low values of stream dynamic pressure. Maximum Mach number capability of the tunnel at various total pressures is shown in figure 34, and typical power requirements for the main-drive motor are shown in figure 35. The Mach number range of the tunnel is from 0.05 to about 0.50, and the unit Reynolds number range is from 0.10×10^6 per foot to about 15.0×10^6 per foot.

TYPICAL AIRFOIL TESTS

Models

Airfoil models tested in the Langley Low-Turbulence Pressure Tunnel completely span the 3-ft-wide test section, and chords of these models range from about 6 in. to 36 in. Models for laminar-flow research usually are constructed with a metal core surrounded by plastic fill with two thin layers of fiberglass forming the aerodynamic surface. The model surface is sanded with No. 400 dry silicon carbide paper to insure an aerodynamically smooth surface. The model contour accuracy is generally within ±0.002 in. Upper- and lower-surface orifices are generally installed with their axes perpendicular to the surface. Multi-element models are constructed of aluminum or steel, and brackets are used to attach flaps or leading-edge devices to the main wing section.

The present model consisted of an NACA 4416 airfoil section with a 35-percent-chord slotted flap. A sketch of the model mounted in the tunnel is shown in figure 36, and a photograph of the model in the tunnel is shown in figure 37. The model was machined from an aluminum billet and had a flap-nested chord of 24 in. and a span of 36 in. The model was equipped with both upper- and lower-surface chordwise rows of orifices located at the midspan ($y/c = 0$) and near the tunnel sidewall ($y/c = 0.625$). Spanwise orifices were located on the upper surface of both the main element and flap in order to monitor the two-dimensionality of the flow.

Methods

The lift, pitching-moment, and drag characteristics of single-element airfoils tested in the Langley Low-Turbulence Pressure Tunnel are determined from pressure

measurements. The static-pressure measurements at the airfoil surface are reduced to standard pressure coefficients and machine integrated to obtain section lift and pitching-moment coefficients. The drag is obtained from measurements of static and total pressures in the wake of the airfoil with a wake survey rake. Section profile-drag coefficients are computed by the method reported in reference 4. For airfoils without pressure orifices and for multi-element airfoils, the section data are obtained from a three-component strain-gage balance. For the present tests, both pressure measurements and force measurements were used to obtain section data.

Corrections

Airfoil data obtained in the Langley Low-Turbulence Pressure Tunnel are corrected for wind-tunnel boundary effects according to reference 4. Corrections for solid and wake blockage are applied to the free-stream dynamic pressure, and corrections for the effects of floor and ceiling constraint on streamline curvature are applied to lift, pitching-moment, and angle of attack. The magnitudes of these corrections for the NACA 4416 airfoil with a chord length of 2 ft are

$$\alpha \text{ corrected} = \alpha + 0.133(c_l + 4c_m)$$

$$c_l \text{ corrected} = c_l(0.976 - 0.134c_d)$$

$$c_m \text{ corrected} = c_m(0.990 - 0.134c_d) + 0.0037c_l$$

$$c_d \text{ corrected} = (0.986 - 0.134c_d)c_d$$

These boundary corrections are considered sufficiently accurate for ratios of model chord to tunnel height ≤ 0.40, and there are no large amounts of boundary-layer flow separation present on the airfoil.

Results

Single-element airfoil.- Section data which are typical for airfoils tested in the Langley Low-Turbulence Pressure Tunnel are shown in figure 38. Results are shown for the NACA 4416 airfoil with the flap in the nested position (gap unsealed). The airfoil was tested both in the smooth condition (natural transition) and with roughness located on both upper and lower surfaces. The roughness was sparsely distributed and consisted of granular-type strips, 0.05 in. wide, which were attached to the surfaces with clear lacquer. Effects of Reynolds number on the section characteristics for the NACA 4416 airfoil are shown in figure 39. A comparison of the present test results for the NACA 4416 airfoil with those of the NACA 4415 airfoil (ref. 5) obtained in the same tunnel about 40 years ago is illustrated in figure 40. Excellent agreement between the lift and pitching-moment data is shown. Comparison of the drag data for the two airfoils indicates higher drag coefficients for the NACA 4416 airfoil at all lift coefficients. The model surface orifices for the NACA 4416 airfoil of this test were located at the center span of the model, which was also the span station where the profile drag measurements were made, whereas the NACA 4415 model of reference 5 had no orifices. Surface roughness effects (early boundary-layer transition) may have resulted from the presence of the orifices. Also, the flap gap was not sealed for the NACA 4416 model.

Multi-element airfoil.- Results for the NACA 4416 airfoil with a 35-percent-chord slotted flap deflected 30° are shown in figures 41 through 43. To insure

two-dimensionality of the flow field for flapped airfoils at high-lift coefficients, tunnel sidewall boundary-layer control (BLC) is provided by tangential blowing of high-pressure air through slots (see fig. 36) located on the model end plates. (The BLC system is described in the "Modifications" section.) Slot blowing is applied until the chordwise pressure data obtained at the model midspan ($y/c = 0.0$) are approximately matched with the chordwise pressure data obtained 3 in. from the tunnel sidewall ($y/c = 0.625$). Typical pressure data for the NACA 4416 slotted-flap model are shown in figure 41 for an angle of attack of 12°. Without BLC, the flow on the flap near the tunnel sidewall is separated. With BLC, the flow on the flap is attached, and the pressure data at the model midspan are approximately matched with the pressure data near the tunnel sidewall. Note also the improvement in the uniformity of the spanwise pressure data on both the wing and flap with BLC. The results of integration of the chordwise pressure data at both span stations ($y/c = 0.0$ and $y/c = 0.625$) to obtain lift and pitching-moment data are illustrated in figure 42. With BLC, the lift and pitching-moment data at both span stations are approximately matched. The drag data shown in the figure were obtained from the strain-gage balance because the unsteadiness of the wake at a flap deflection of 30° precluded an accurate determination of drag using the wake survey method. Figure 43 shows a comparison between the integrated pressure data and force-balance data without BLC. Good agreement is shown for both lift and pitching-moment data between the balance data and the integrated pressure data at the midspan station.

CONCLUDING REMARKS

The Langley Low-Turbulence Pressure Tunnel is a single-return, closed-throat tunnel which can be operated at stagnation pressures from near vacuum to 10 atm. The test section is rectangular in shape, 3 ft wide, 7.5 ft high, and 7.5 foot long. The Mach number range of the tunnel is from 0.05 to about 0.50, and the unit Reynolds number range is from 0.10×10^6 per foot to about 15.0×10^6 per foot. Recent modifications to the approximately 40-year-old facility included the following: replacement of the original cooling coils and antiturbulence screens and addition of a tunnel-shell heating system, a two-dimensional model-support and force-balance system, a sidewall boundary-layer control system, a remote-controlled survey apparatus, and a new data-acquisition system. Also, a calibration of the mean flow parameters in the test section was conducted. The primary conclusions are as follows:

Test-section turbulence measurements made after replacement of the original cooling coils and antiturbulence screens were about the same as the 1941 measurements. Tangential blowing of high-pressure air through slots located on the model end plates (sidewall boundary-layer control) eliminated flow separation at the flap and sidewall juncture and is required to obtain useful results from two-dimensional tests of high-lift multi-element airfoils.

The calibration of the mean flow parameters in the test section over the operating range of the facility indicated that the flow is uniform between tunnel stations of -40 in. and 40 in. In the test region normally occupied by an airfoil model (-20 in. to 20 in.), the maximum variation in Mach number was about ± 0.50 percent. The maximum variation in dynamic pressure compared with the tunnel reference dynamic pressure was about 0.8 percent and occurred in a small core region near the center of the test section. The maximum flow angularity measured was less than 0.20°. A total-pressure deficit was measured near the center of the test section, and the maximum value of the deficit was about 0.8 percent of the stream dynamic pressure.

Comparison of section data for the NACA 4416 airfoil with data for the NACA 4415 airfoil tested in this same facility about 40 years ago generally showed good agreement.

Langley Research Center
National Aeronautics and Space Administration
Hampton, VA 23665
June 5, 1984

REFERENCES

1. Von Doenhoff, Albert E.; and Abbott, Frank T., Jr.: The Langley Two-Dimensional Low-Turbulence Pressure Tunnel. NACA TN 1283, 1947.

2. Pope, Alan; and Harper, John J.: Low-Speed Wind Tunnel Testing. John Wiley & Sons, Inc., c.1966.

3. Bryer, D. W.; and Pankhurst, R. C.: Pressure-Probe Methods for Determining Wind Speed and Flow Direction. Her Majesty's Stationery Office (London), 1971, pp. 24-25.

4. Pankhurst, R. C.; and Holder, D. W.: Wind-Tunnel Technique. Sir Issac Pitman & Sons, Ltd. (London), 1965.

5. Abbott, Ira H.; Von Doenhoff, Albert E.; and Stivers, Louis S., Jr.: Summary of Airfoil Data. NACA Rep. 824, 1945. (Supersedes NACA WR L-560.)

L-81-1345

Figure 1.- Photograph of Langley Low-Turbulence Pressure Tunnel.

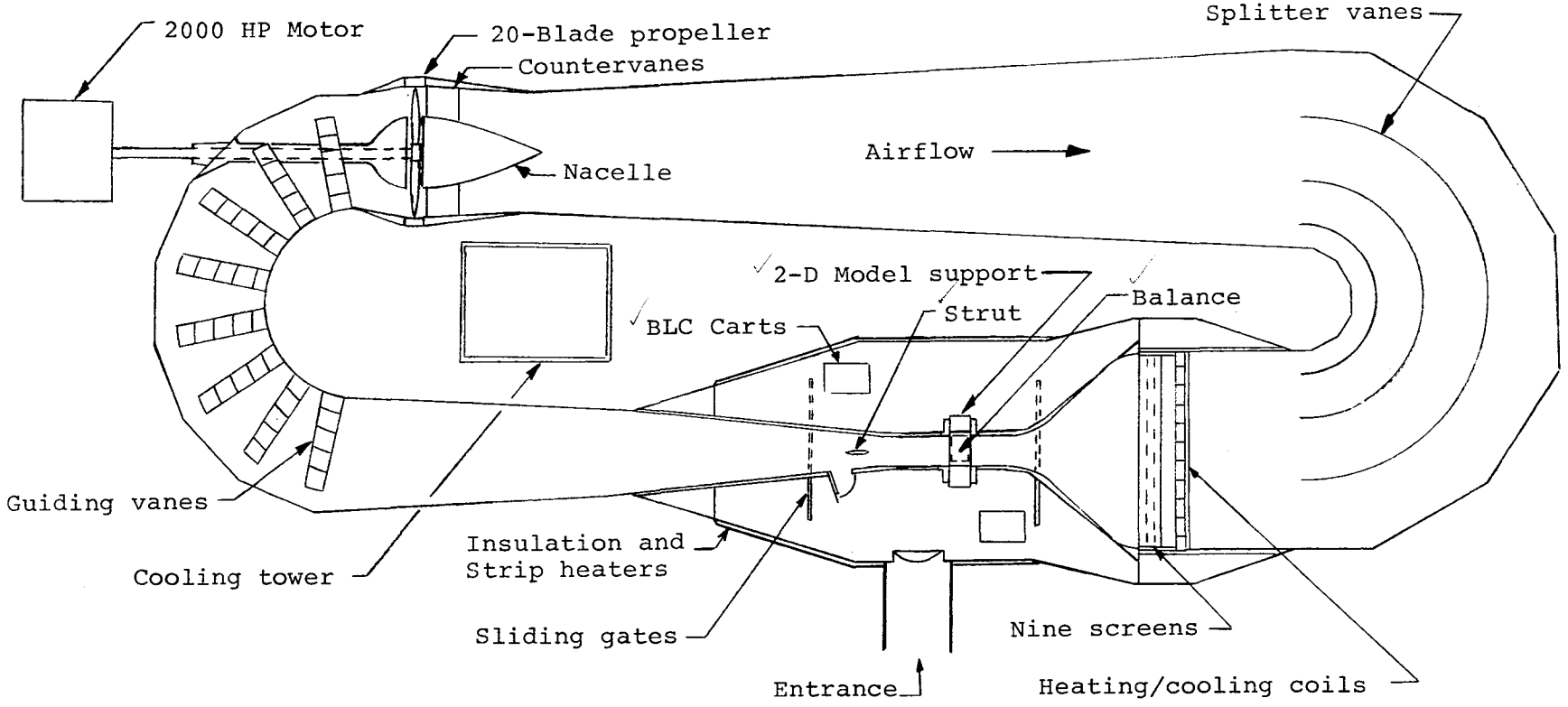

Figure 2.- Sketch of Langley Low-Turbulence Pressure Tunnel circuit arrangement.

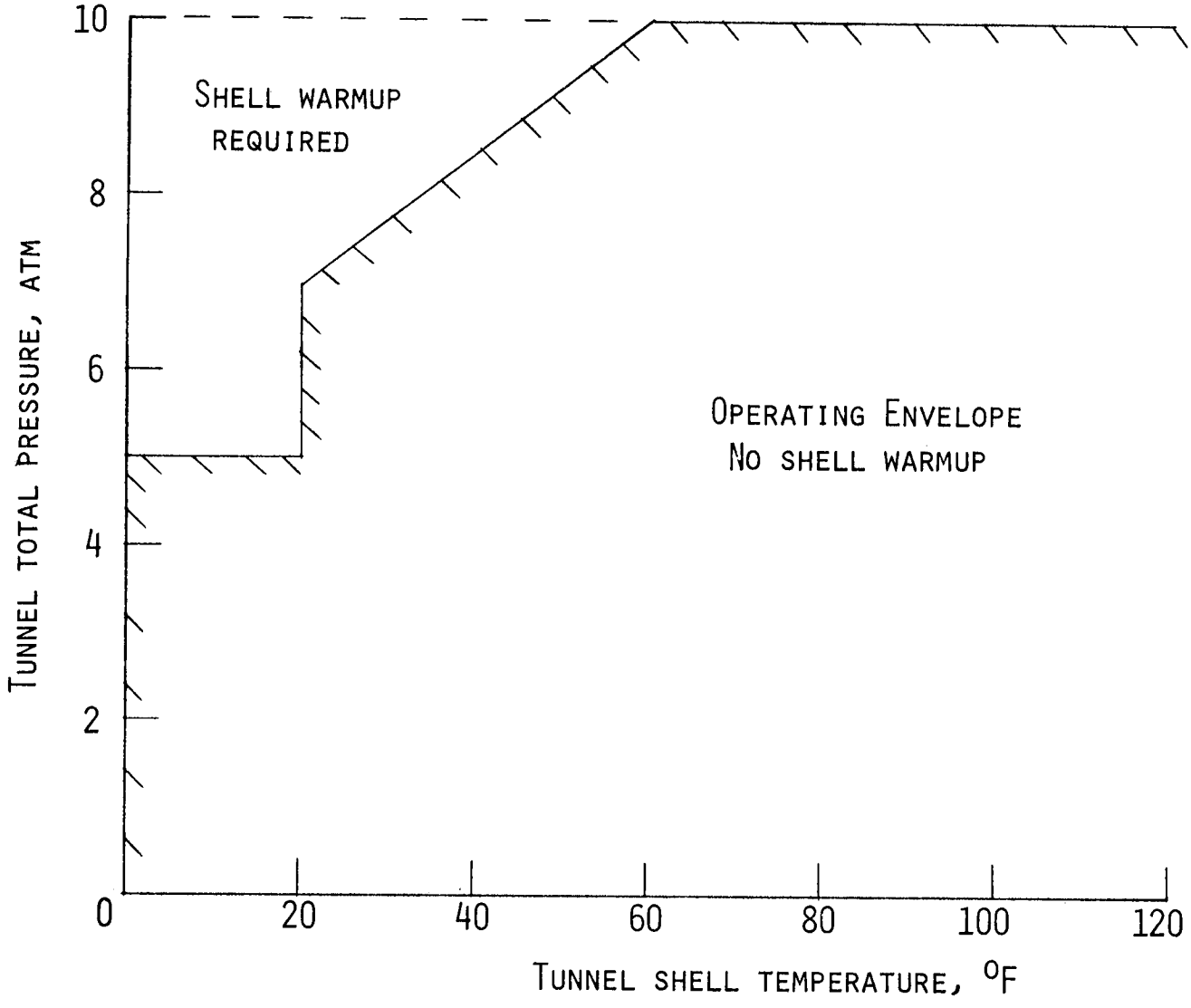

Figure 3.- Pressure-temperature restriction for Langley Low-Turbulence Pressure Tunnel.

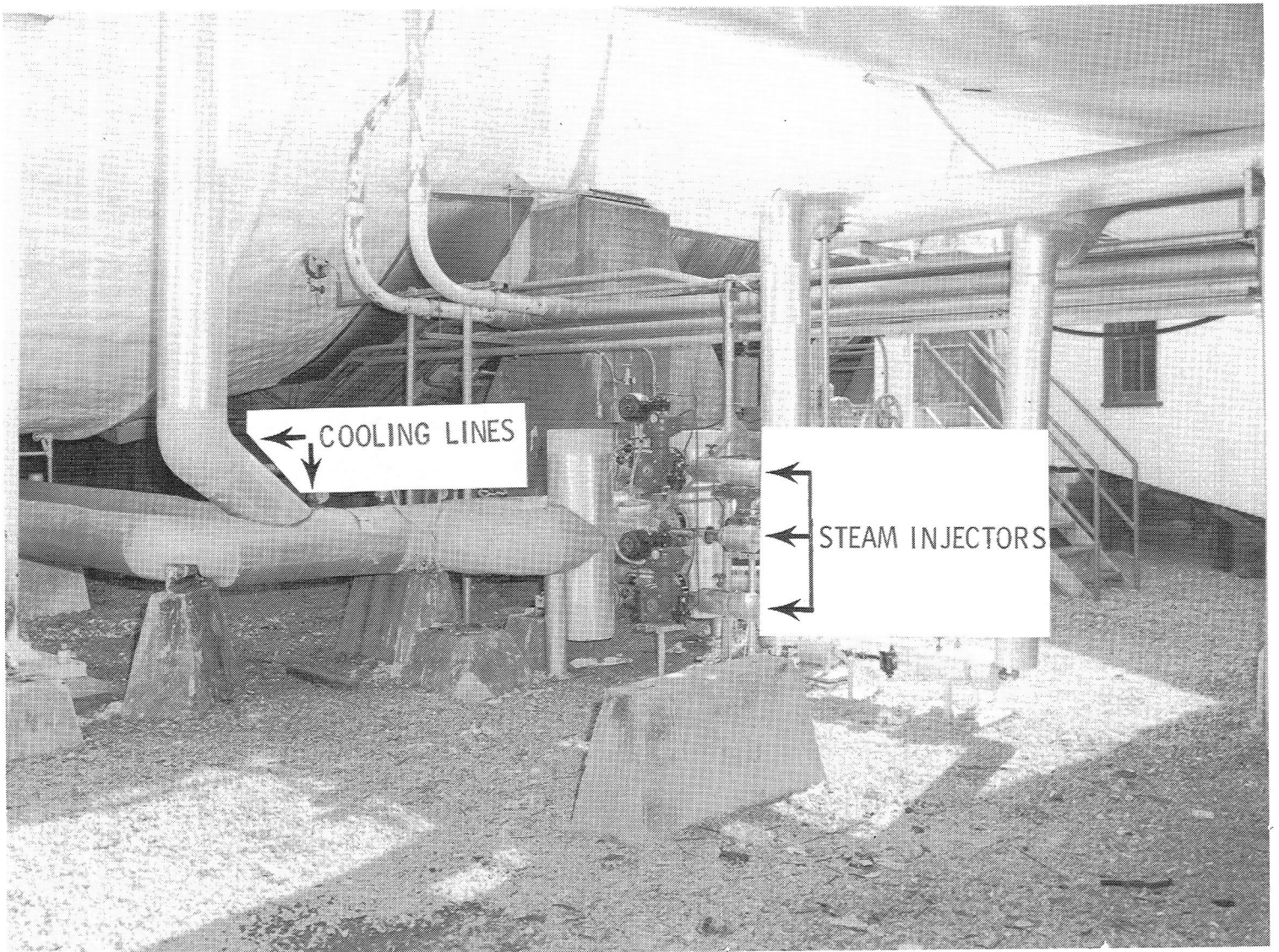

L-81-1346.1

(a) Photograph.

Figure 4.- Cooling lines and steam injectors for automatic temperature control system.

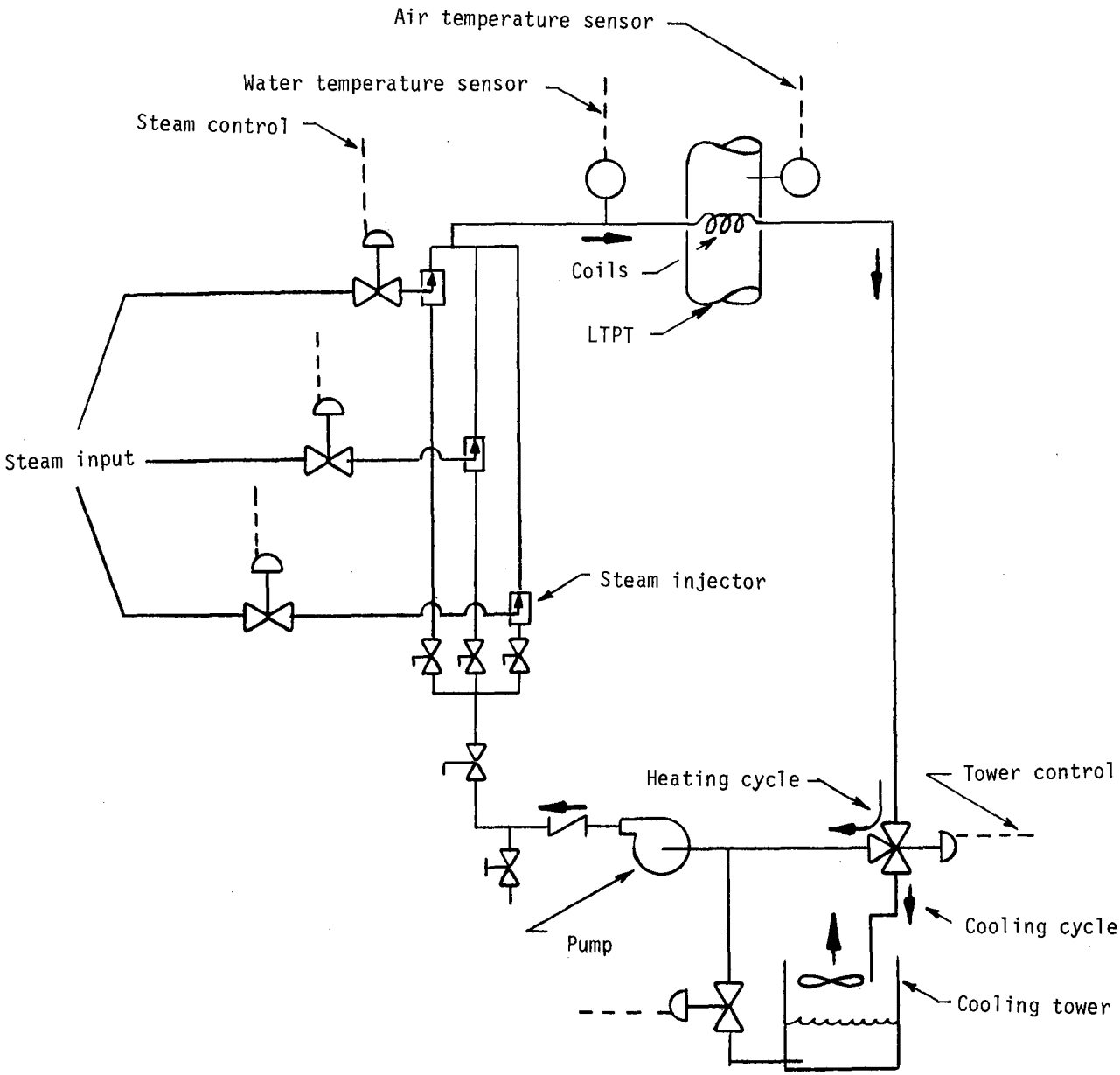

(b) Schematic diagram.

Figure 4.- Concluded.

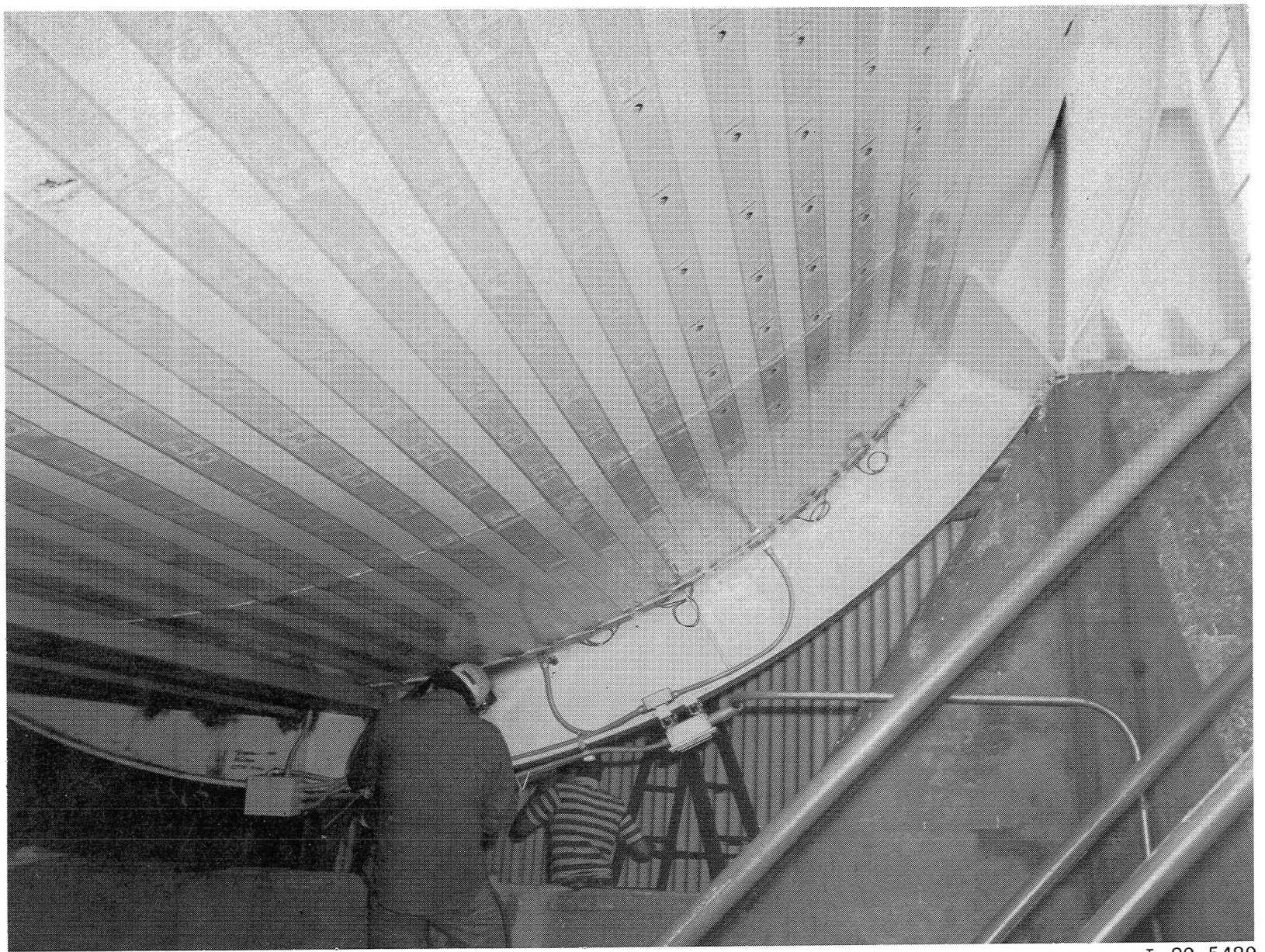

L-80-5489

Figure 5.- Photograph of strip-heater installation on outside shell of test chamber.

L-81-1343

Figure 6.- Photograph of new turbulence-reducing screen installation in Langley Low-Turbulence Pressure Tunnel.

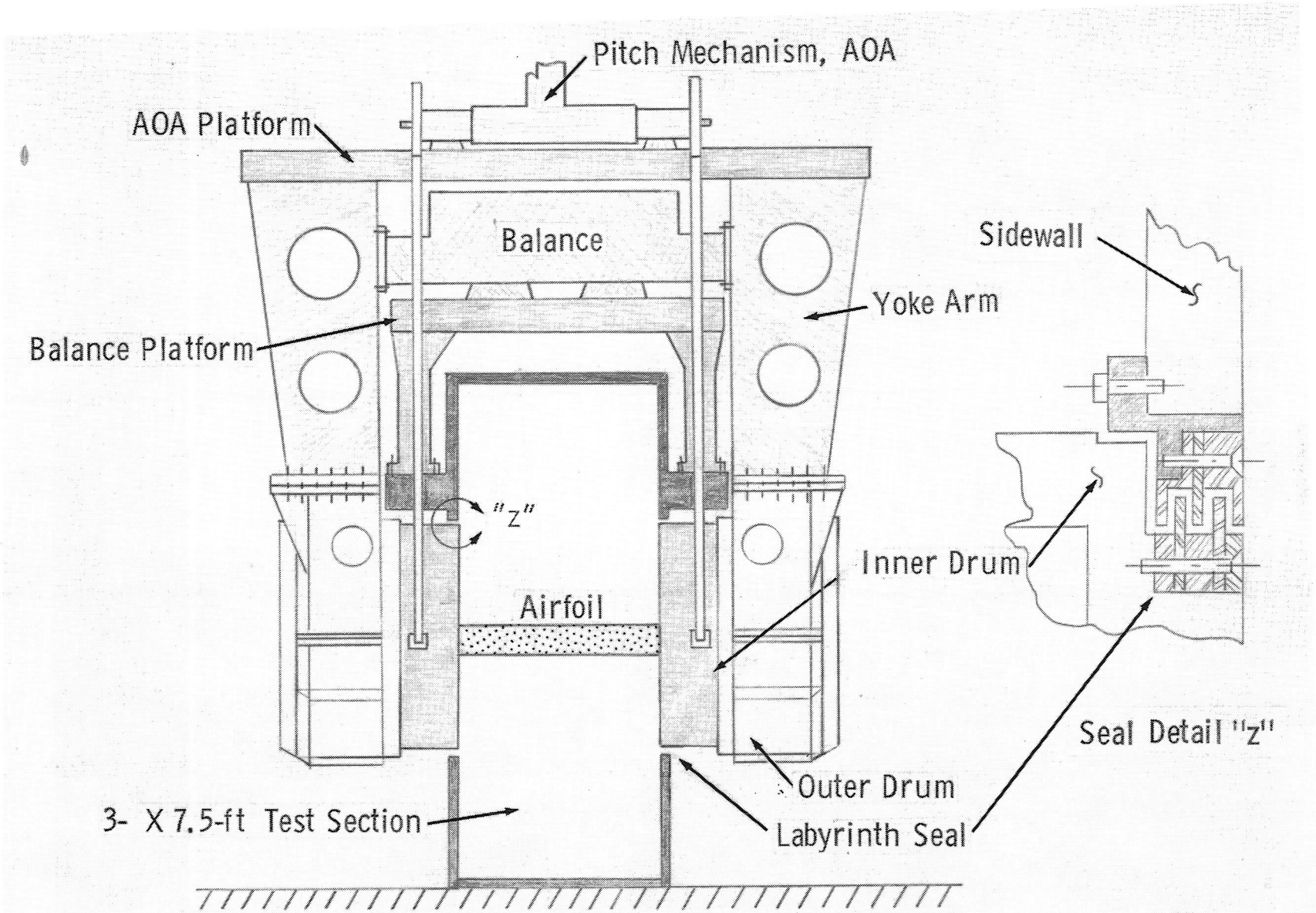

Figure 7.- Model-support and force-balance system for Langley Low-Turbulence Pressure Tunnel (looking upstream).

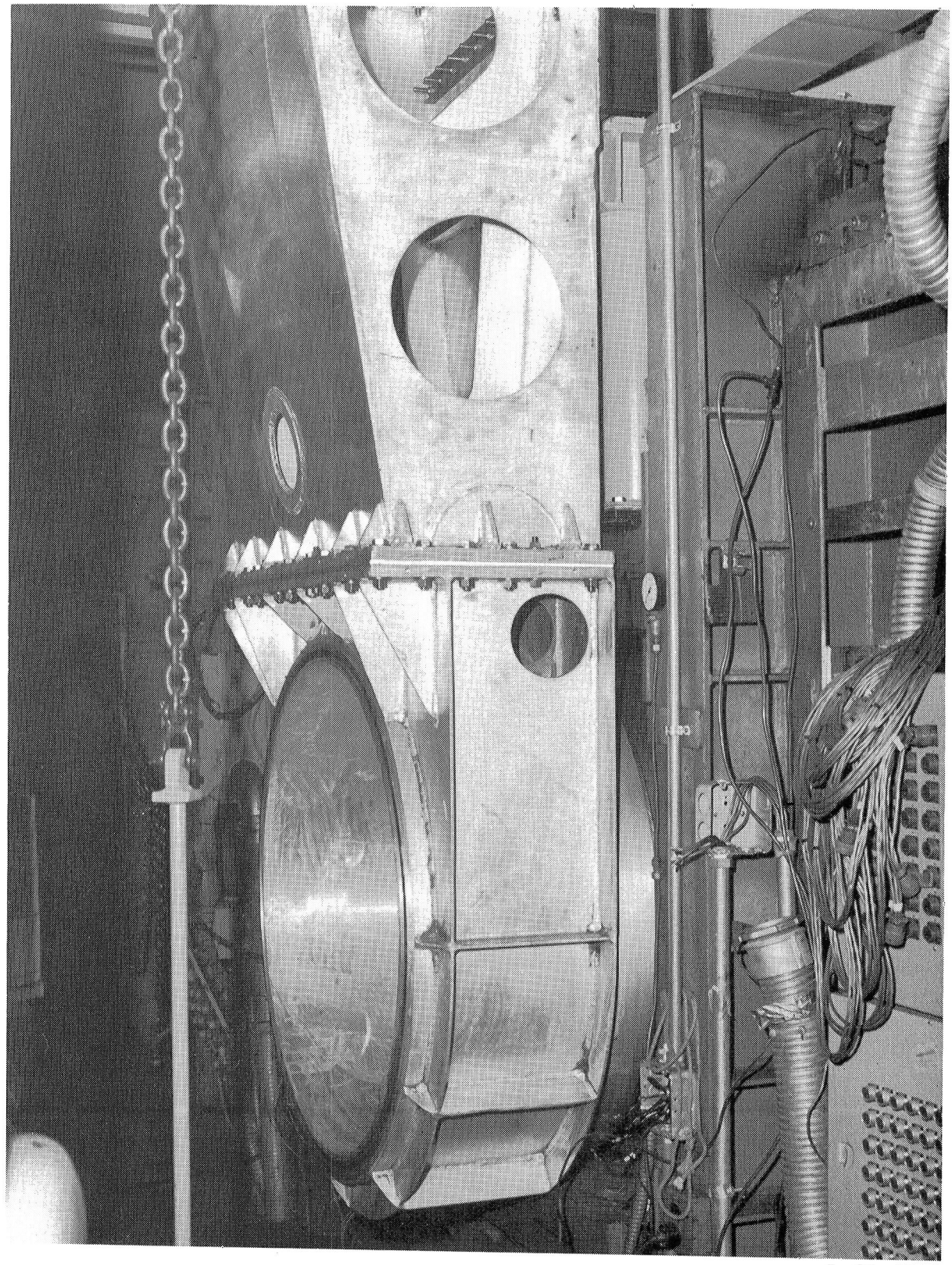

L-81-4516

Figure 8.- Photograph of yoke-arm support system and drum arrangement.

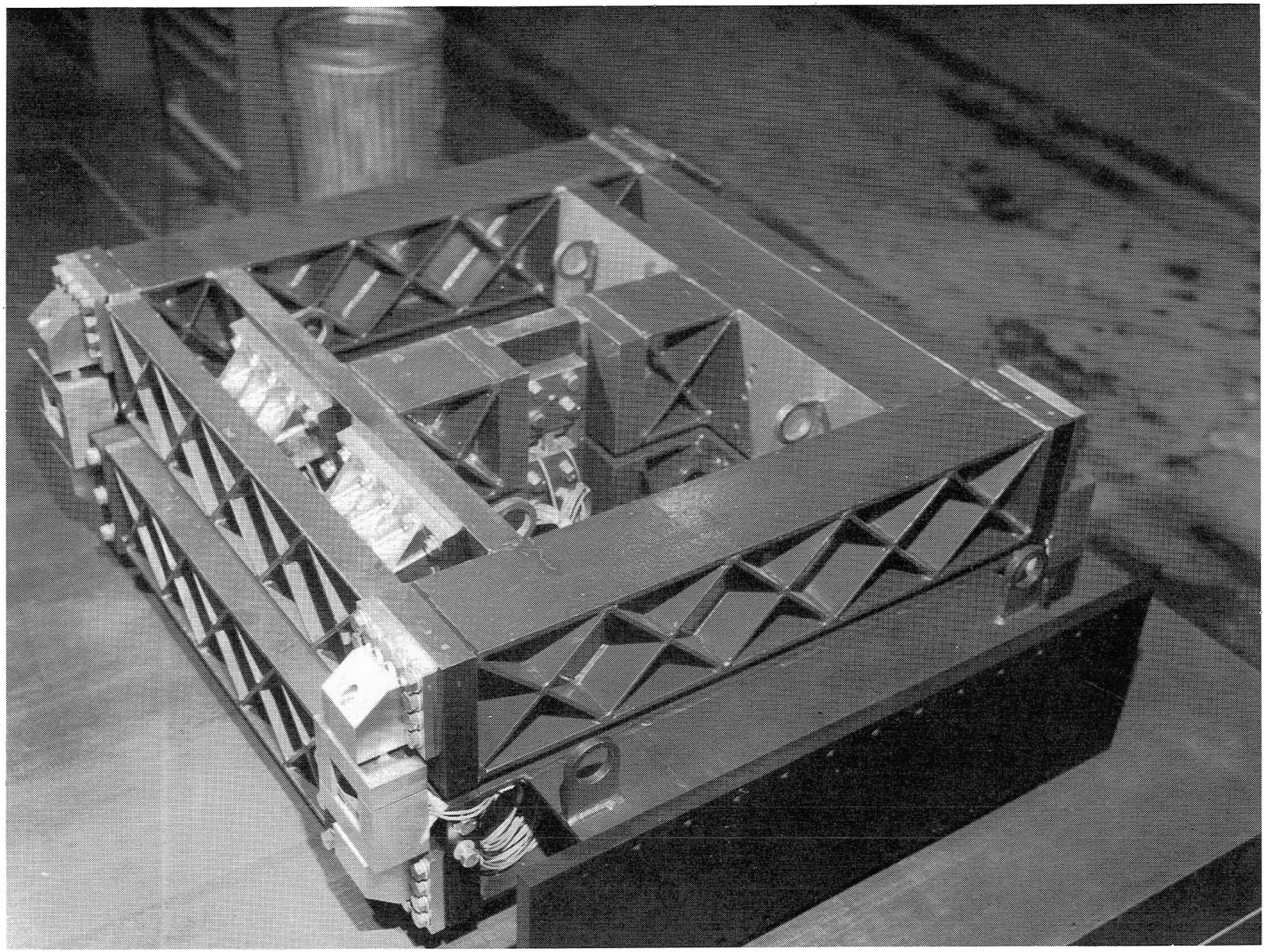

L-79-7037

Figure 9.- Photograph of three-component balance for Langley Low-Turbulence Pressure Tunnel.

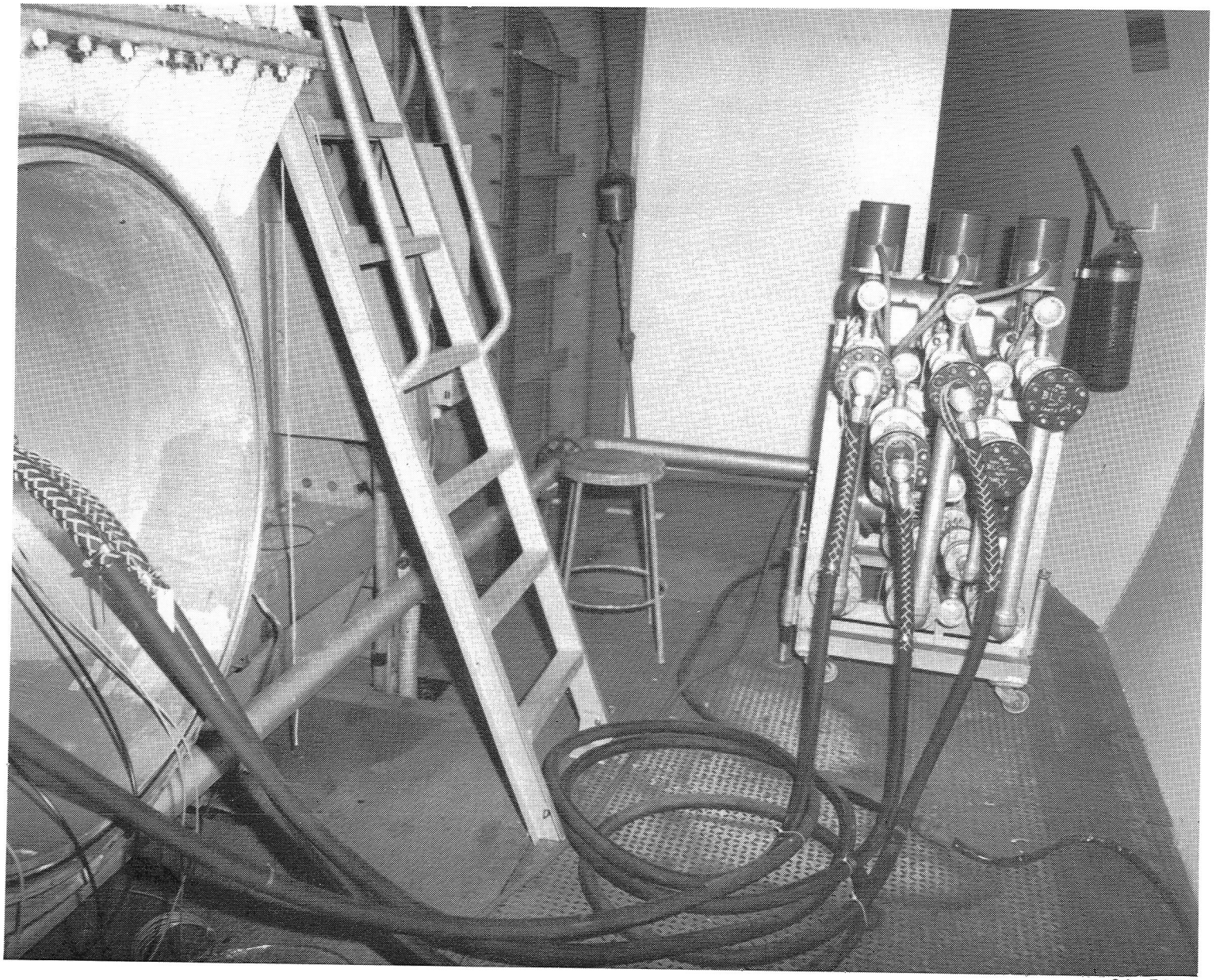

L-82-5996

Figure 10.- Photograph of mobile blowing-box control cart and flexible hoses for sidewall boundary-layer control system.

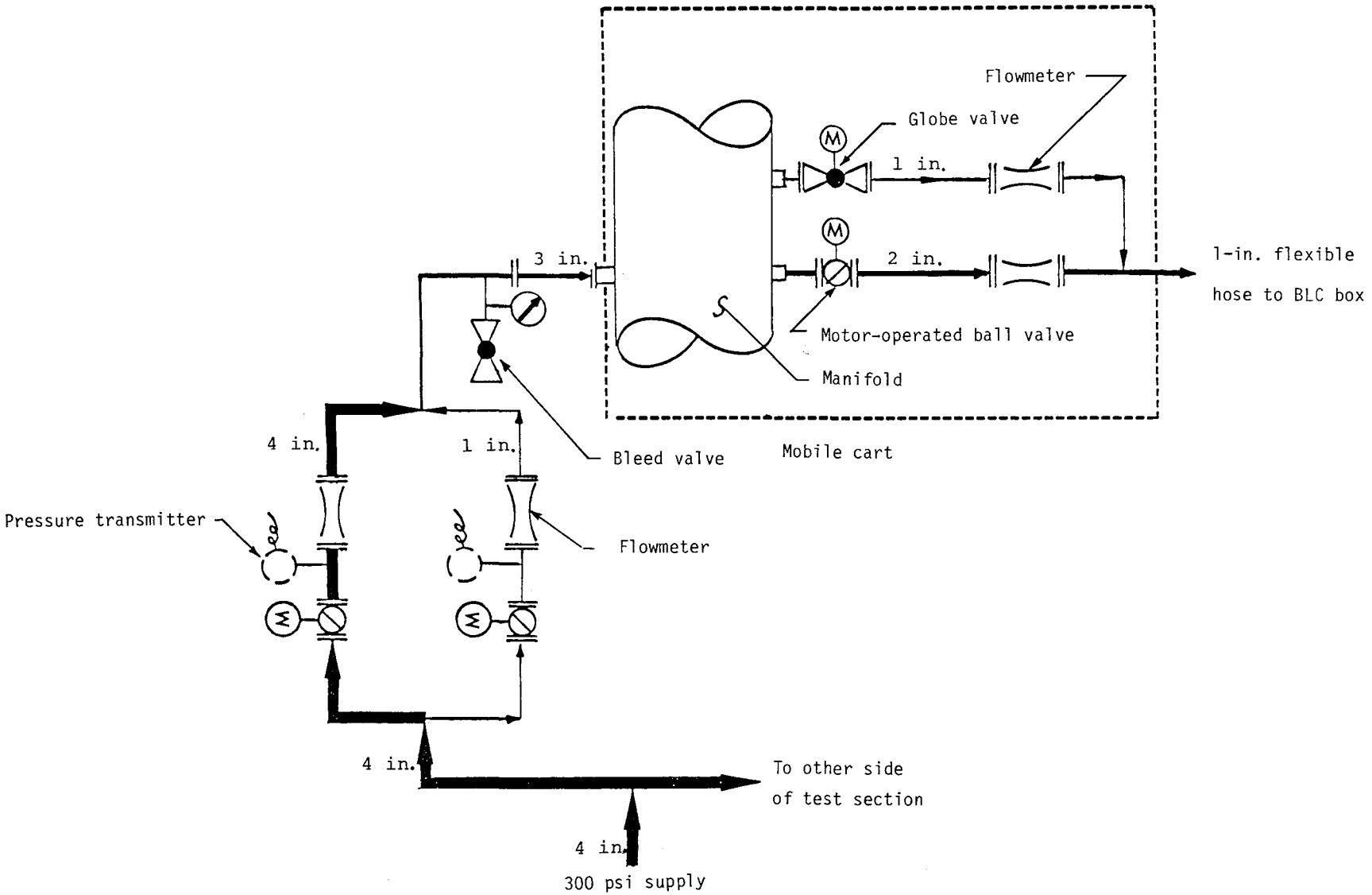

Figure 11.- Schematic of boundary-layer control system for one side of tunnel test section.

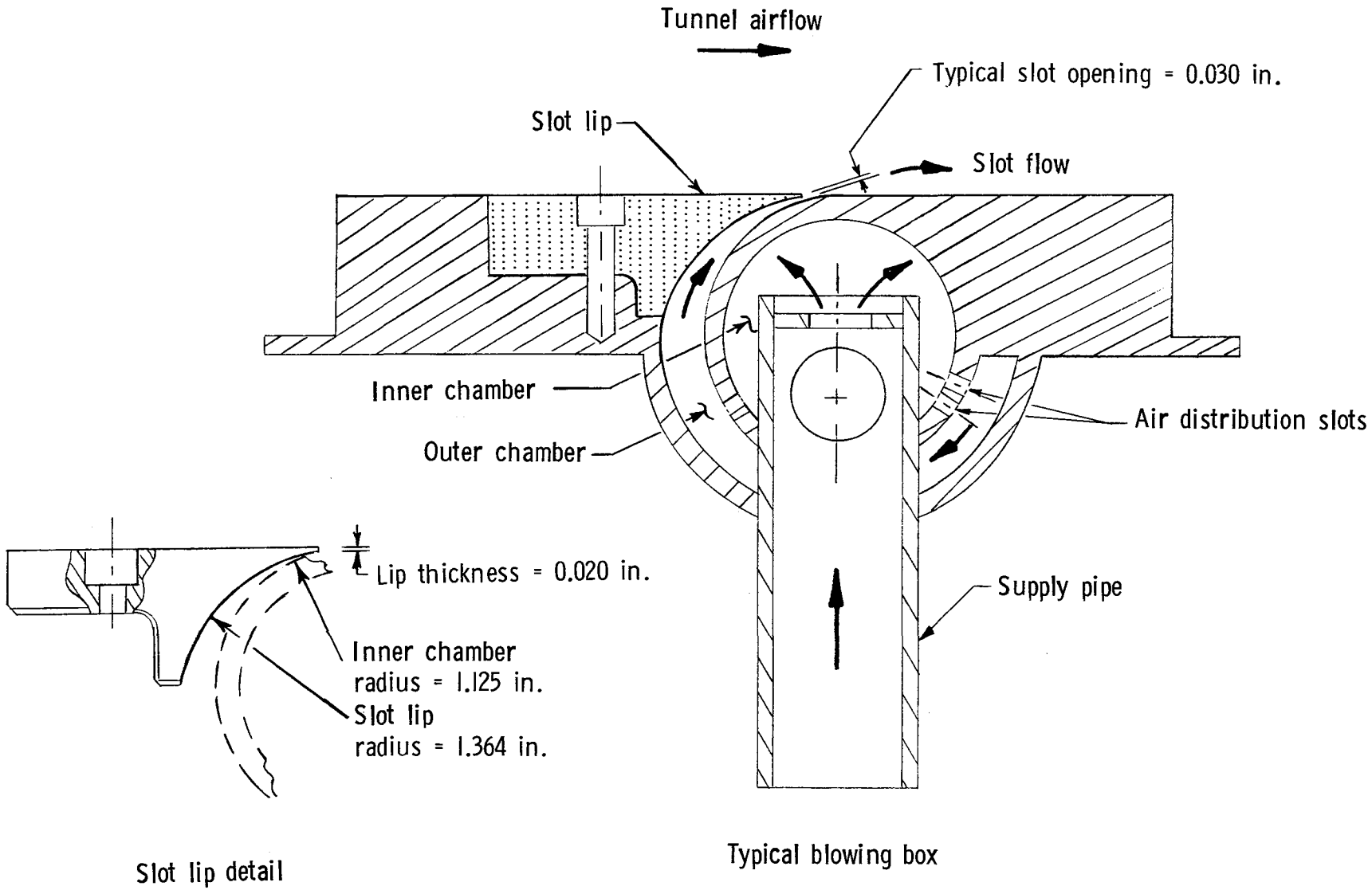

Figure 12.- Sketch of typical blowing-box for sidewall boundary-layer control system.

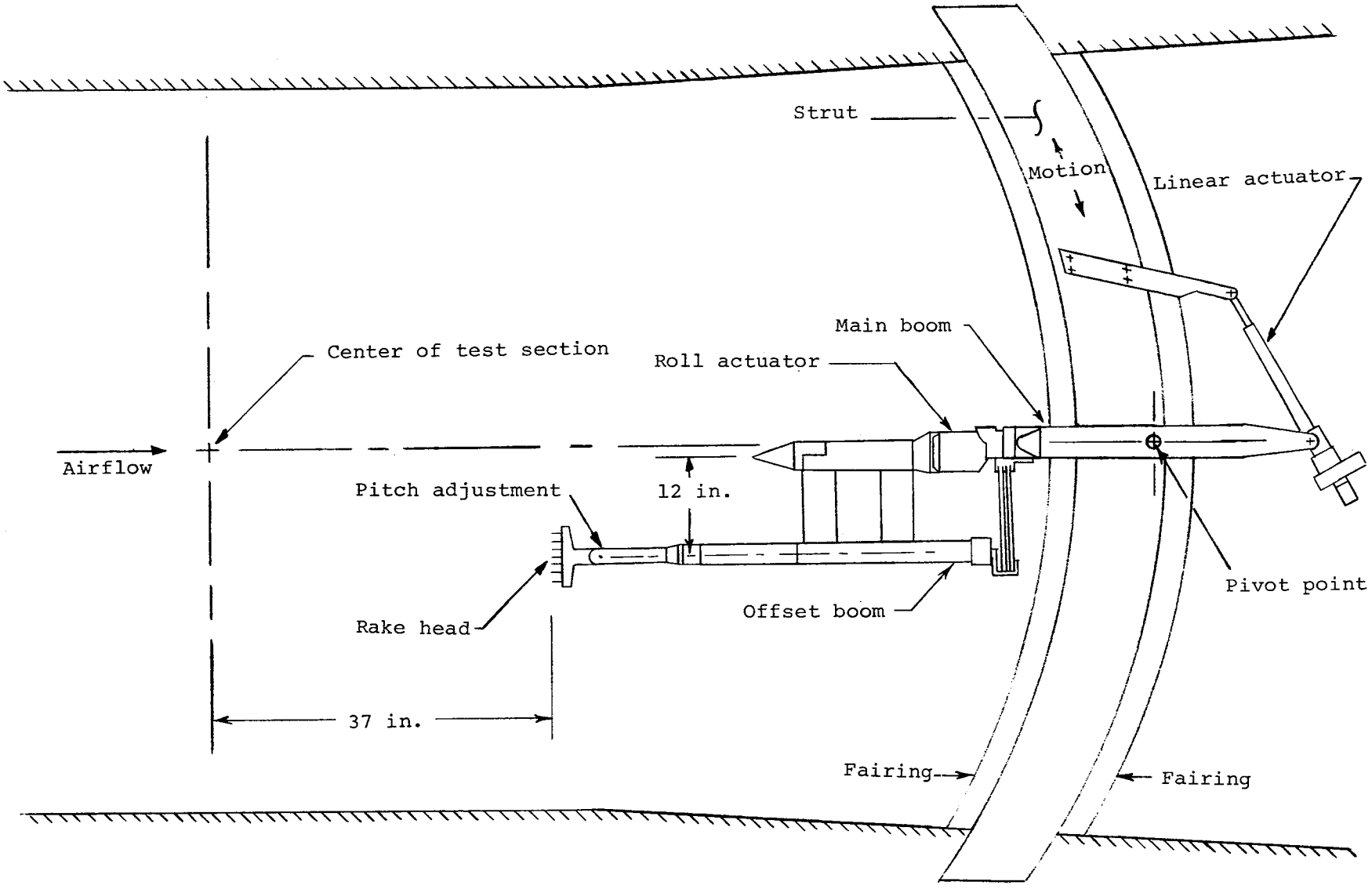

Figure 13.- Sketch of remote-controlled survey apparatus for Langley Low-Turbulence Pressure Tunnel.

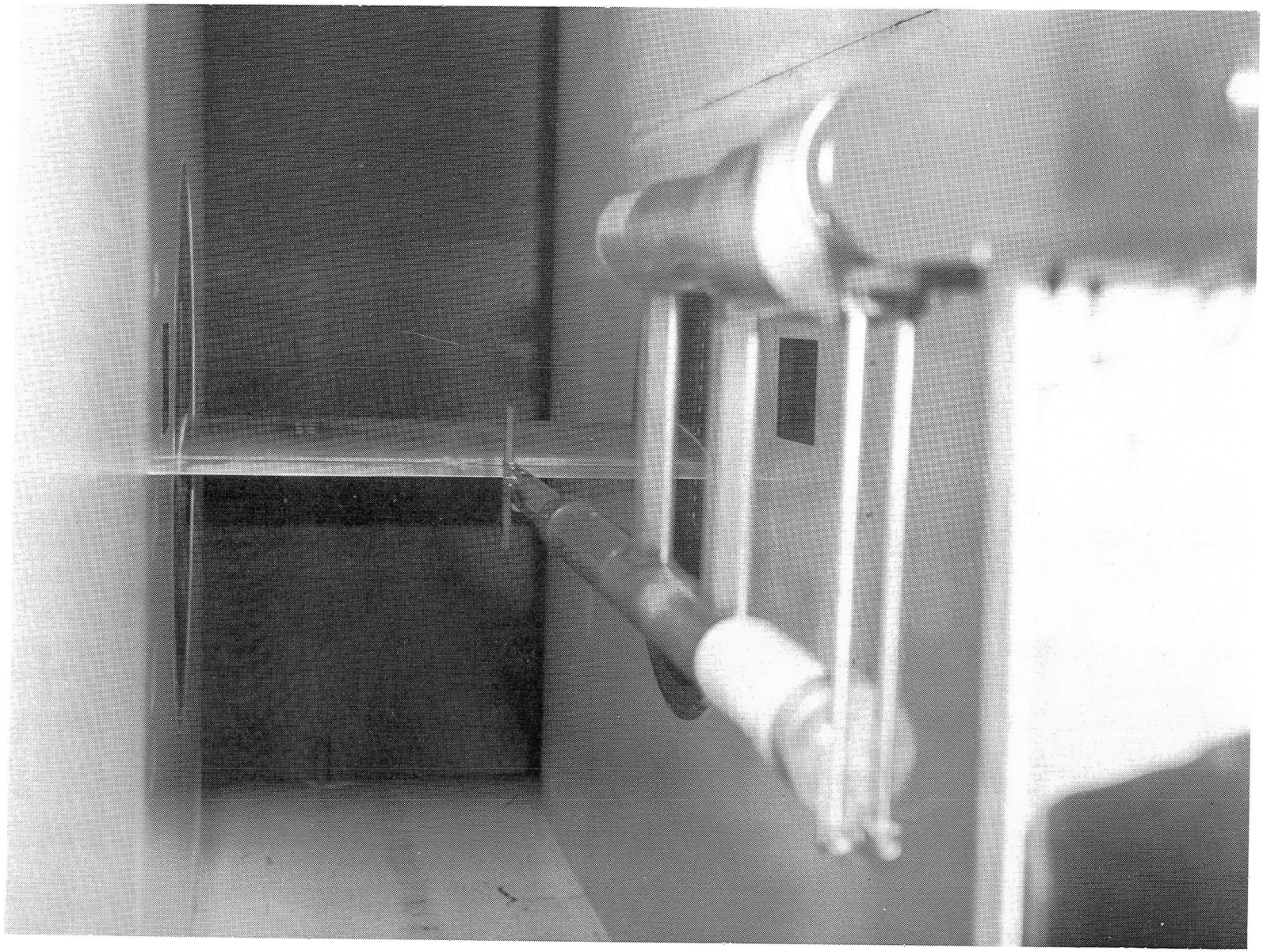

L-83-1134

Figure 14.- Photograph of survey apparatus mounted in Langley Low-Turbulence Pressure Tunnel.

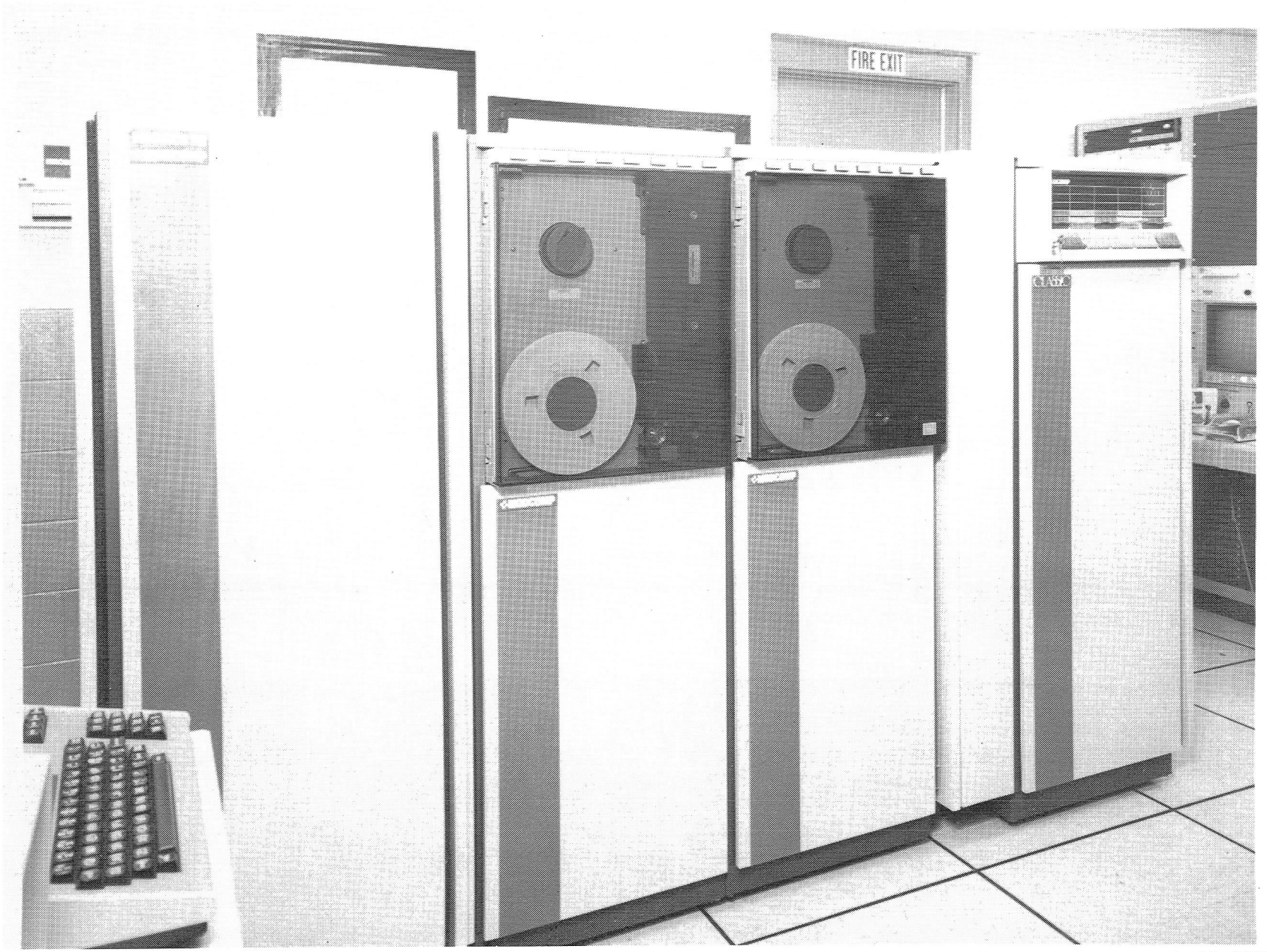

L-80-7599

Figure 15.- Photograph of computer and magnetic tape units for tunnel data-acquisition system.

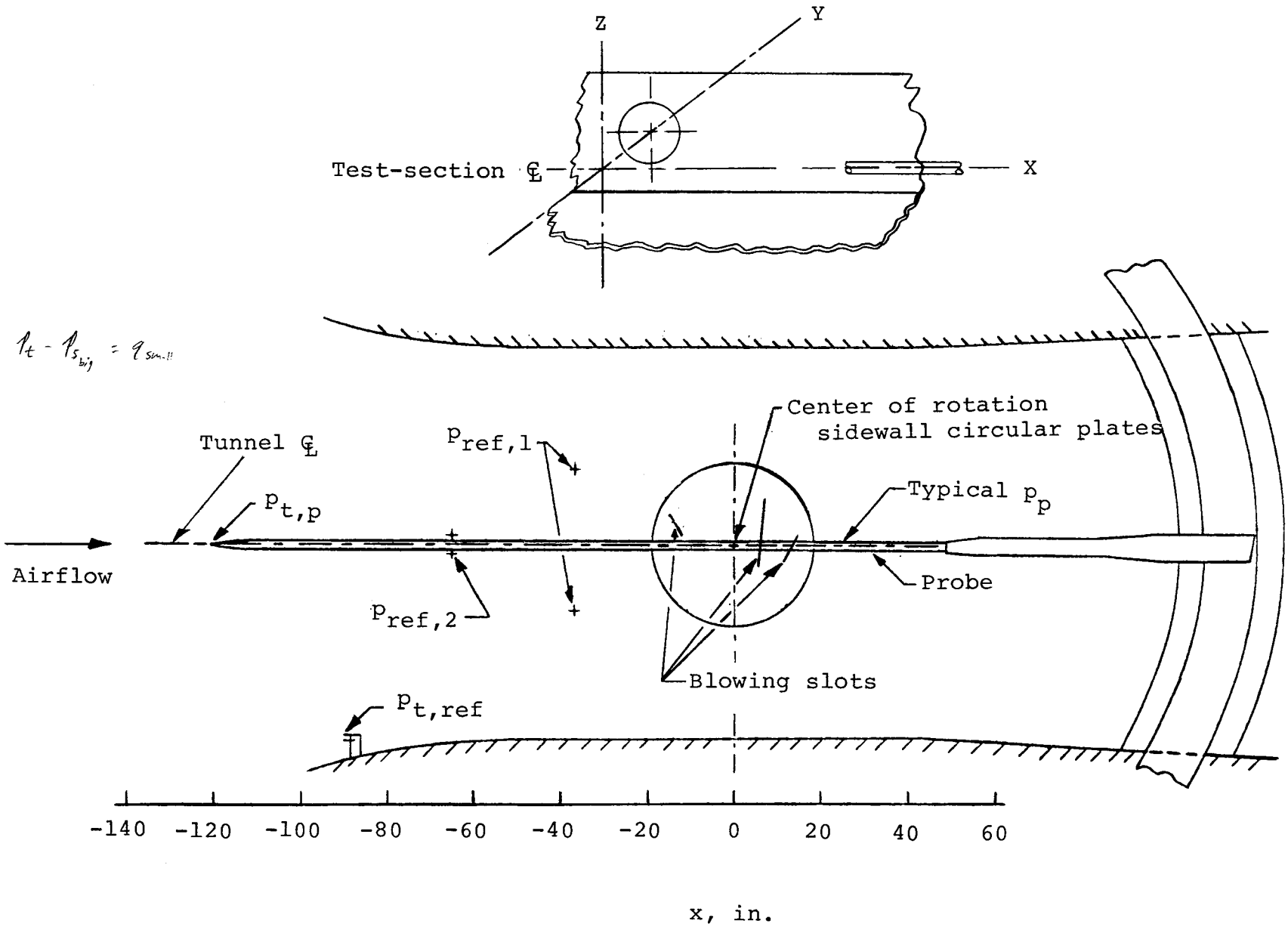

Figure 16.- General calibration arrangement. The symbol + denotes sidewall orifice.

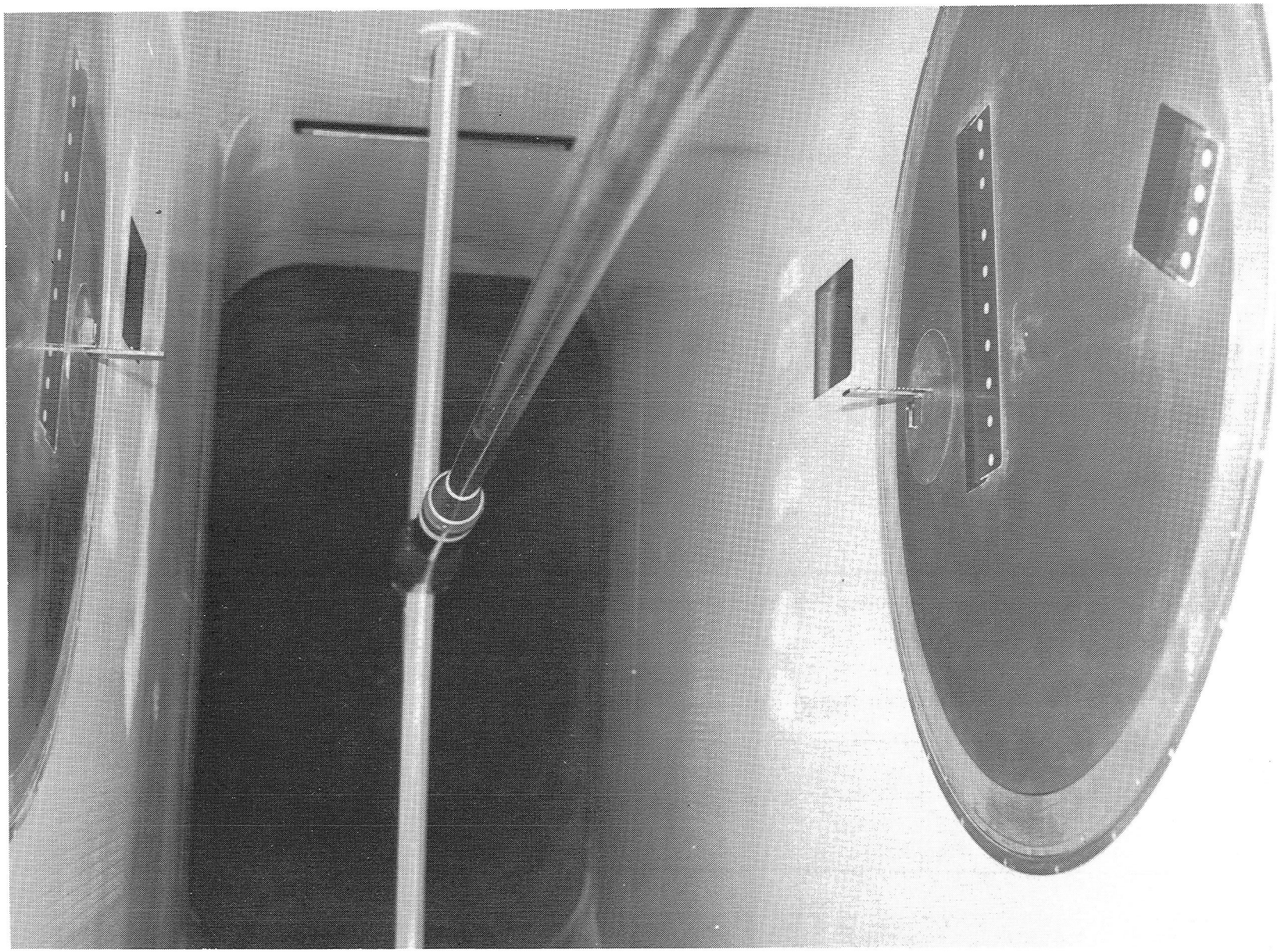

L-82-8494

Figure 17.- Photograph of long survey probe and boundary-layer rake mounted in wind tunnel.

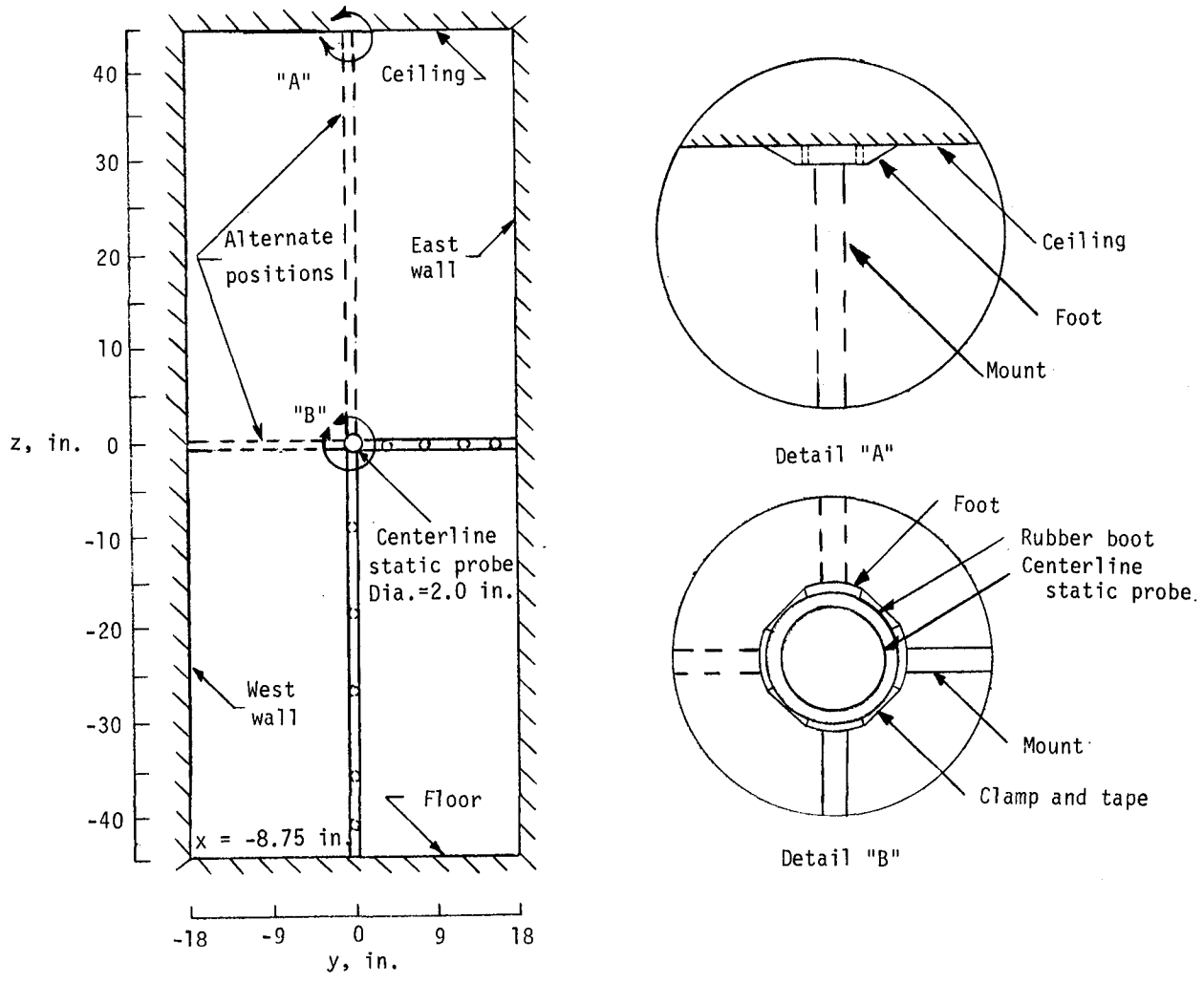

Pitot-static probe arrangement and mount attachment (looking upstream)

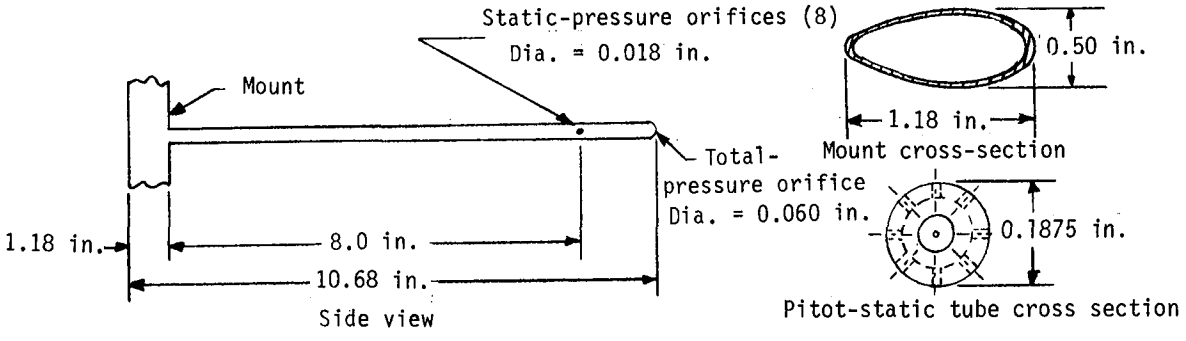

Typical pitot-static probe and mount

(a) Vertical and horizontal rakes of standard pitot-static probes.

Figure 18.- Details of various rakes and probes used in tunnel calibration.

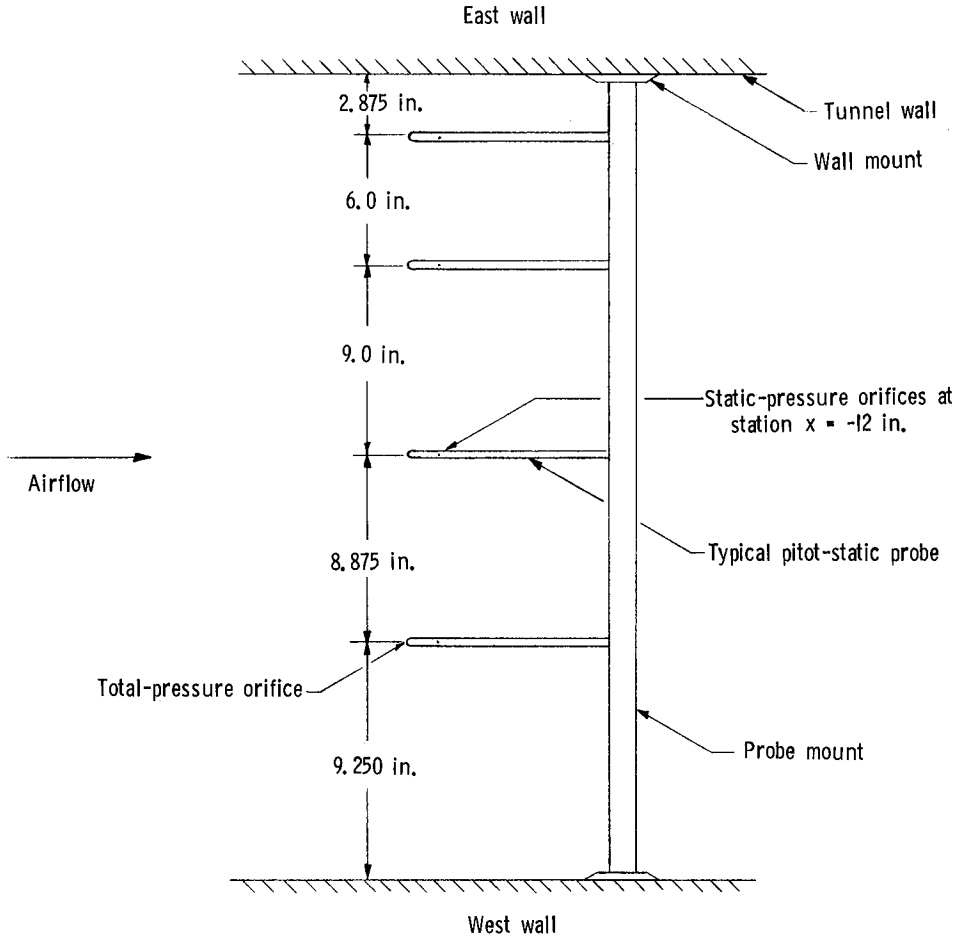

Pitot-static probe arrangement

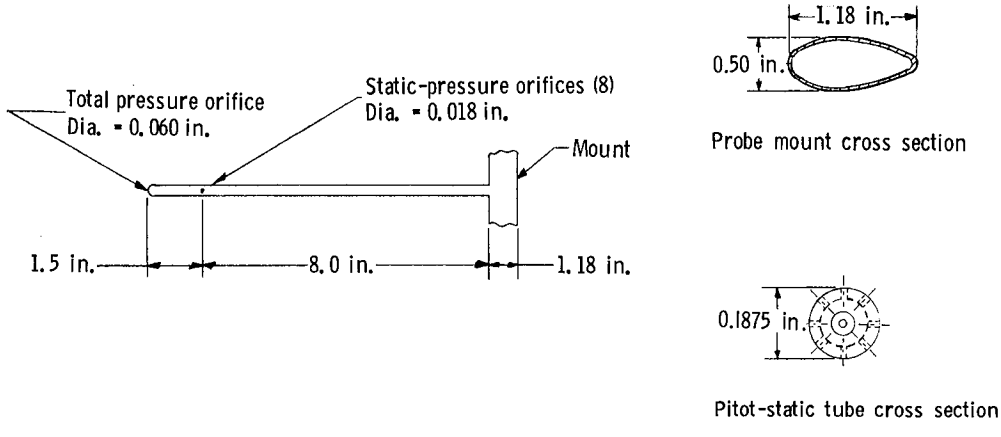

Typical pitot-static probe and mount

(b) Horizontal rake of standard pitot-static probes.

Figure 18.- Continued.

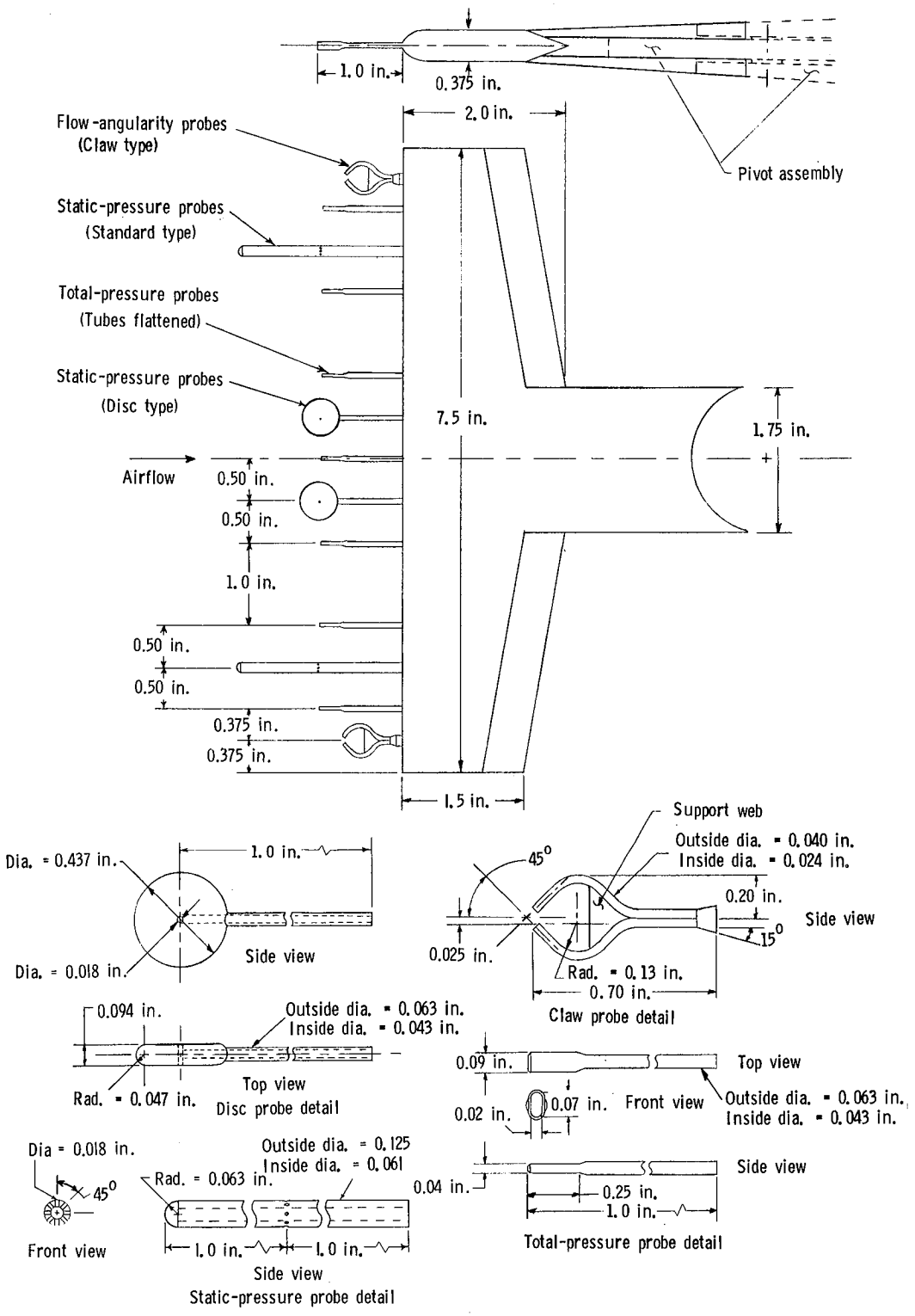

(c) Wake survey rake.

Figure 18.- Continued.

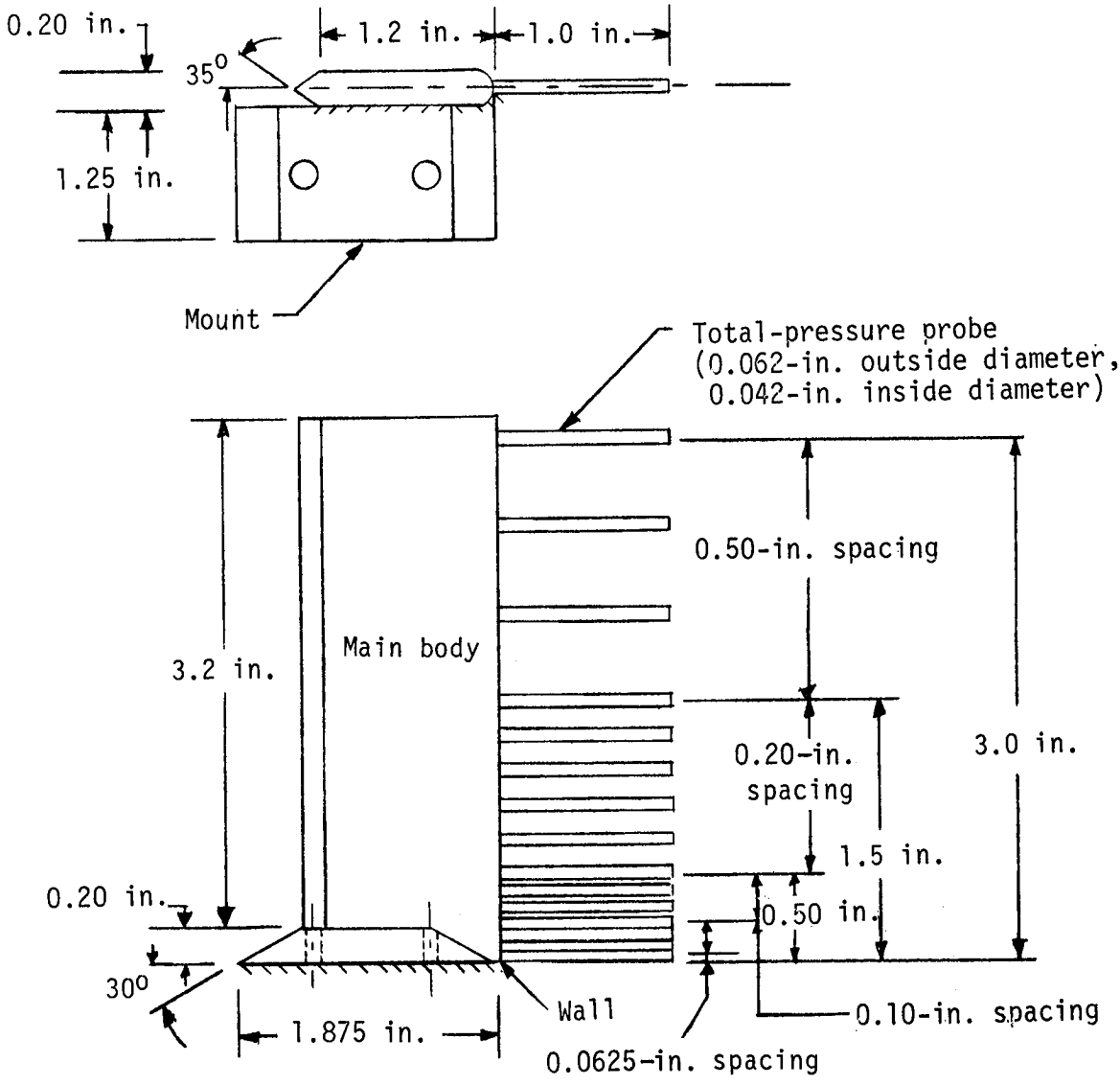

(d) Boundary-layer rake.

Figure 18.- Concluded.

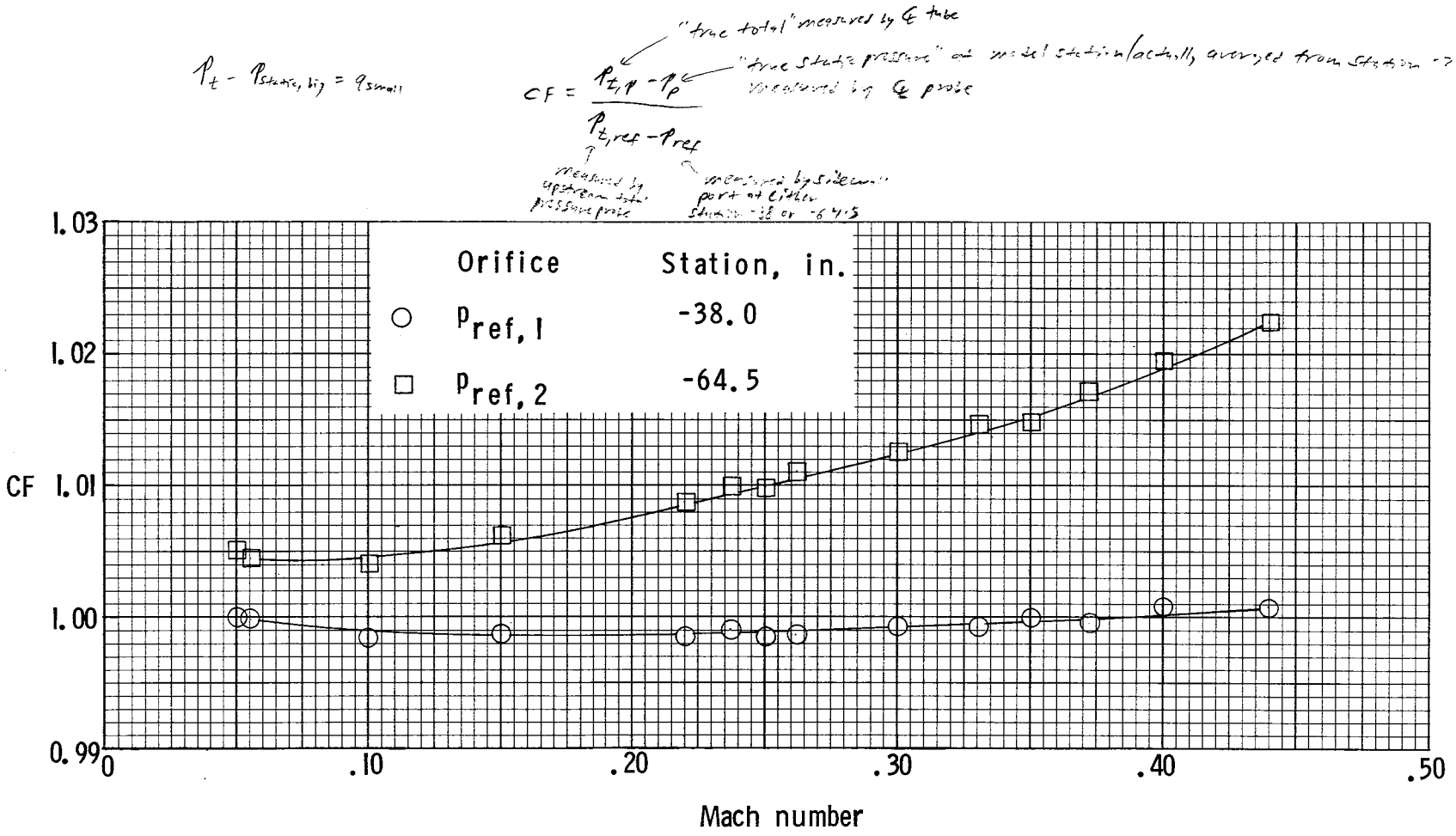

Figure 19.- Calibration factors for Langley Low-Turbulence Pressure Tunnel. Total pressures range from 1 to 10 atm.

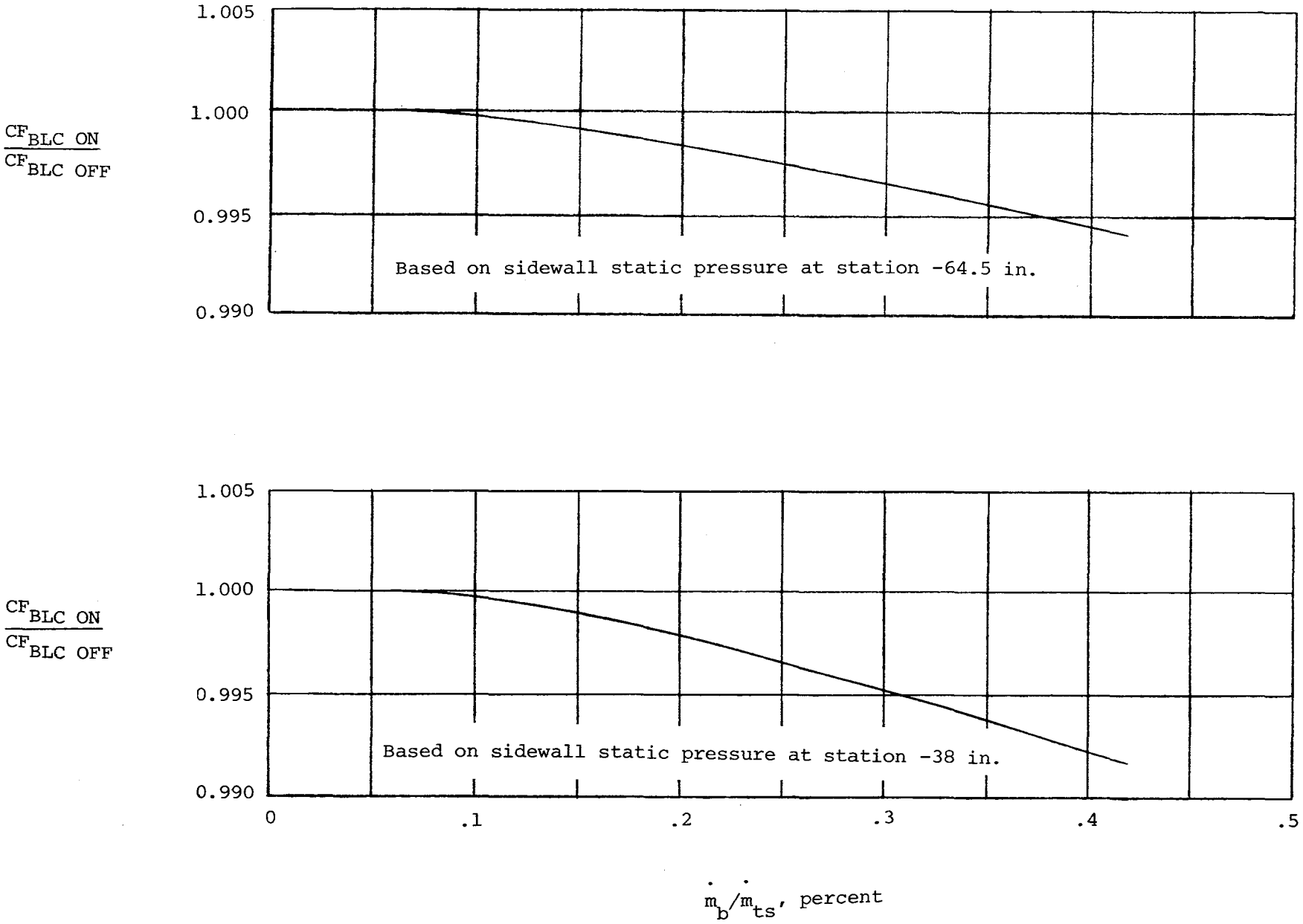

Figure 20.- Effect of tangential blowing (BLC) on tunnel calibration factors.

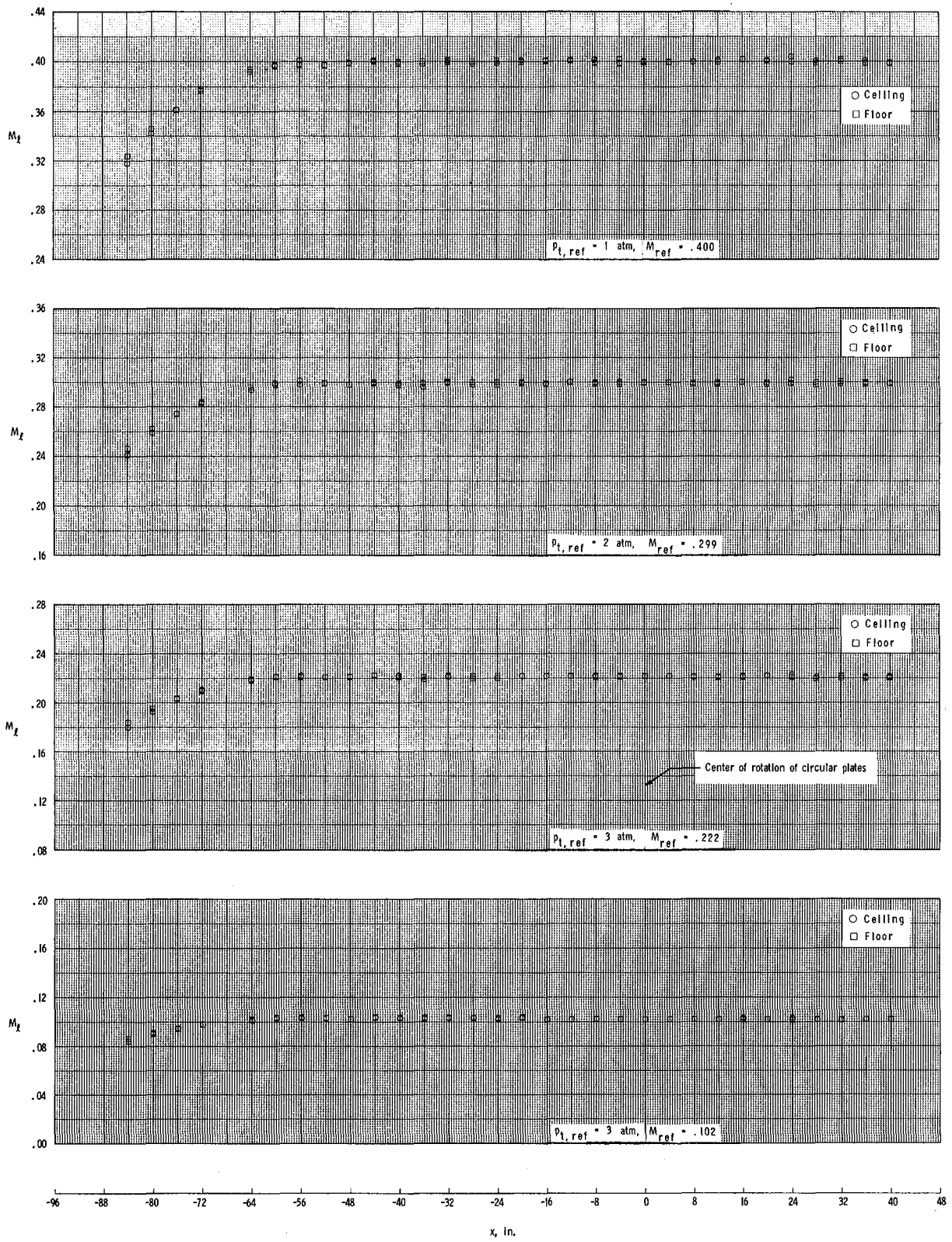

(a) Floor and ceiling.

Figure 21.- Typical Mach number distributions for Langley Low-Turbulence Pressure Tunnel.

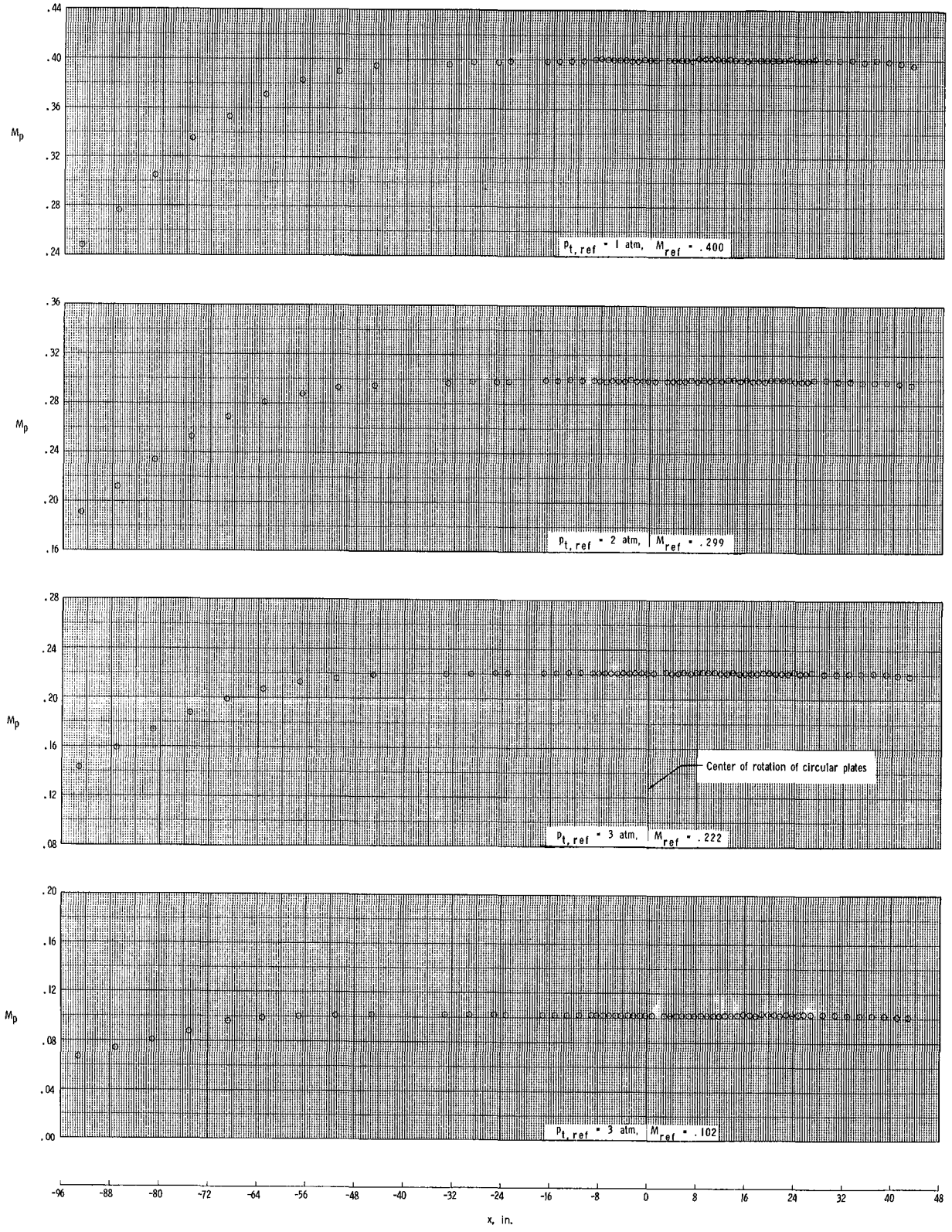

(b) Centerline.

Figure 21.- Continued.

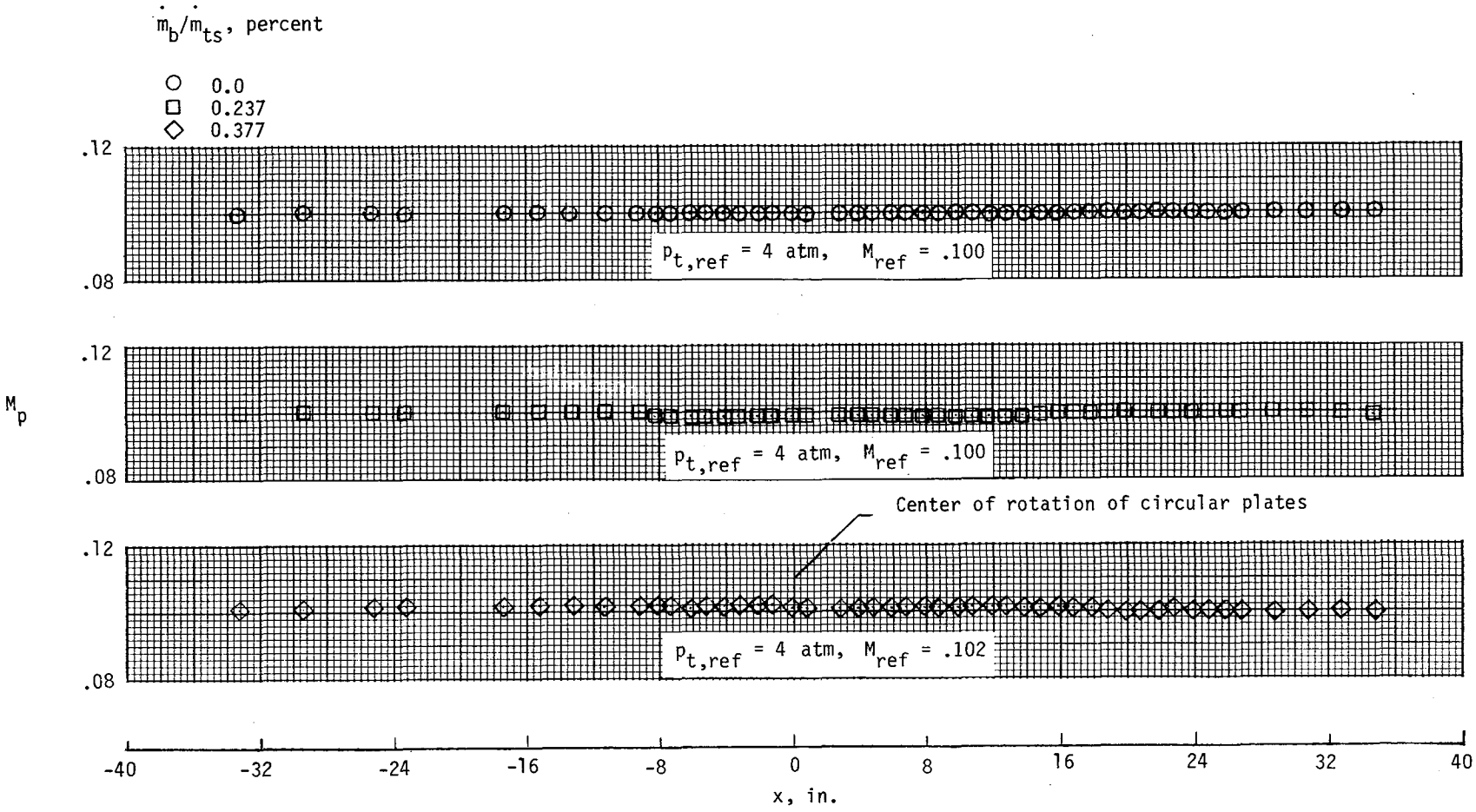

(c) Centerline with and without sidewall boundary-layer control.

Figure 21.- Concluded.

L-82-9000

Figure 22.- Photograph of vertical and horizontal rakes of standard pitot-static probes mounted in wind tunnel.

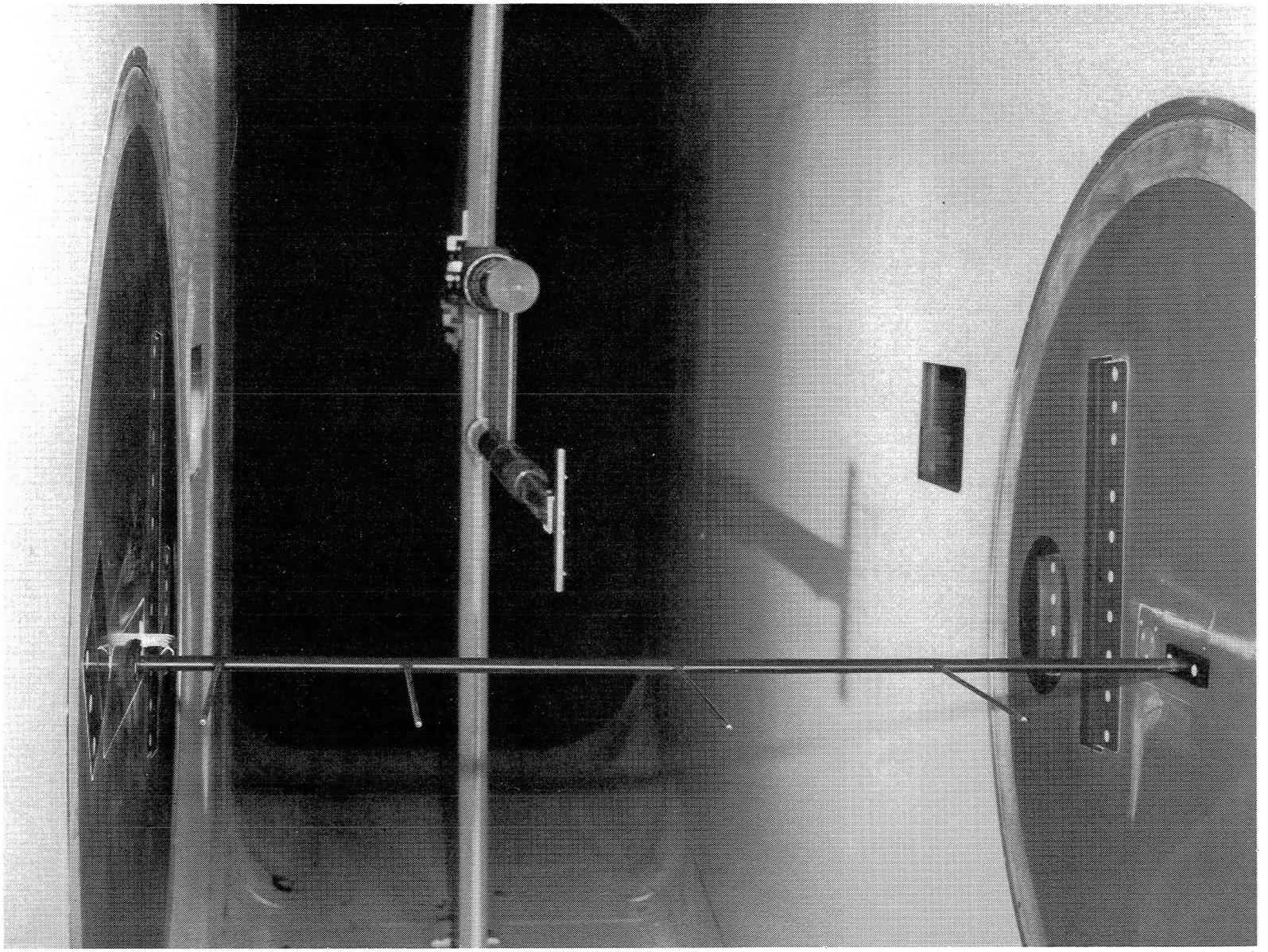

L-82-11,839

Figure 23.- Photograph of horizontal rake of standard pitot-static probes mounted in wind tunnel.

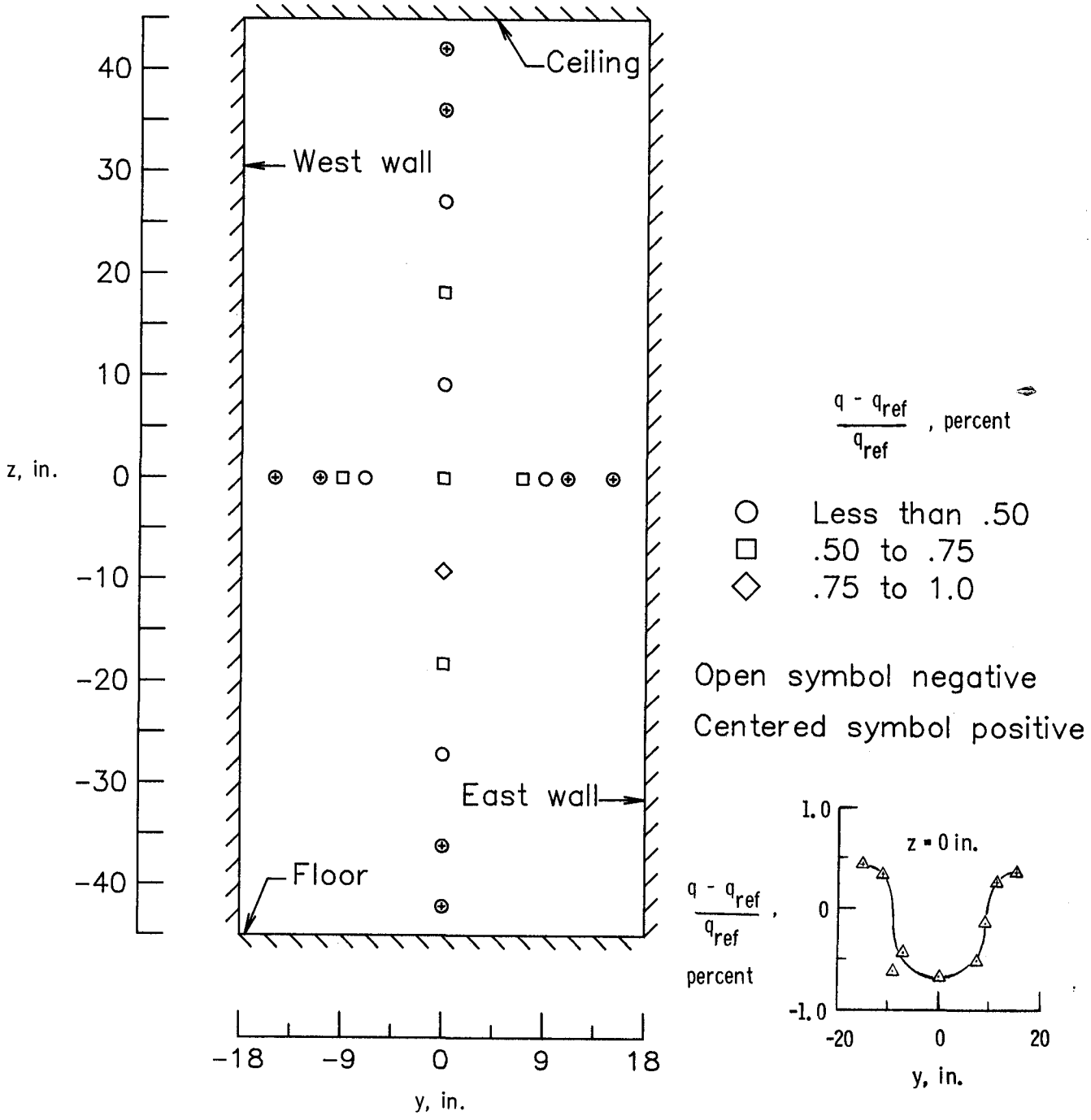

Figure 24.- Typical cross-sectional dynamic-pressure variations. x varies from about -9 in. to -12 in.

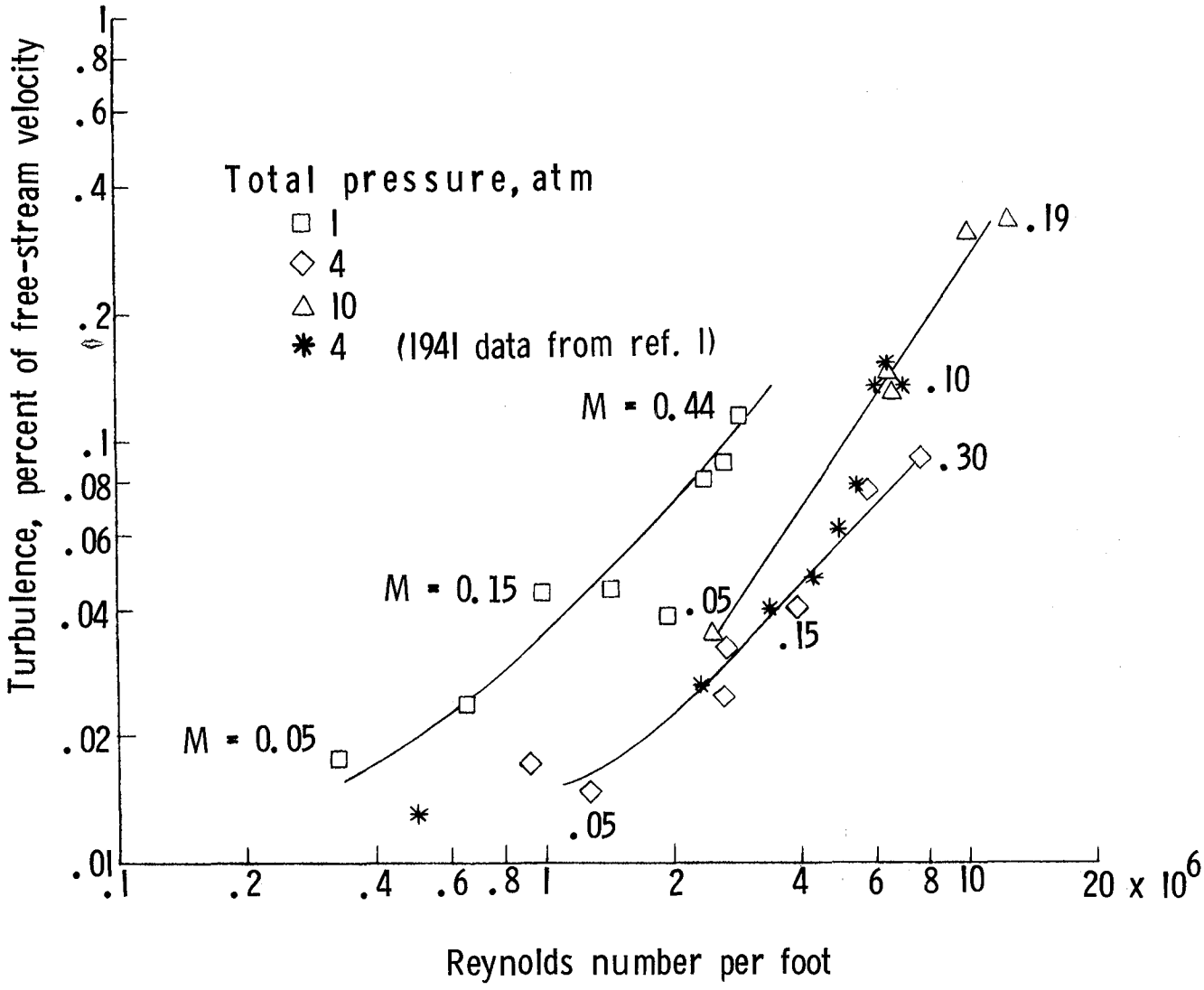

Figure 25.- Test-section turbulence levels of Langley Low-Turbulence Pressure Tunnel.

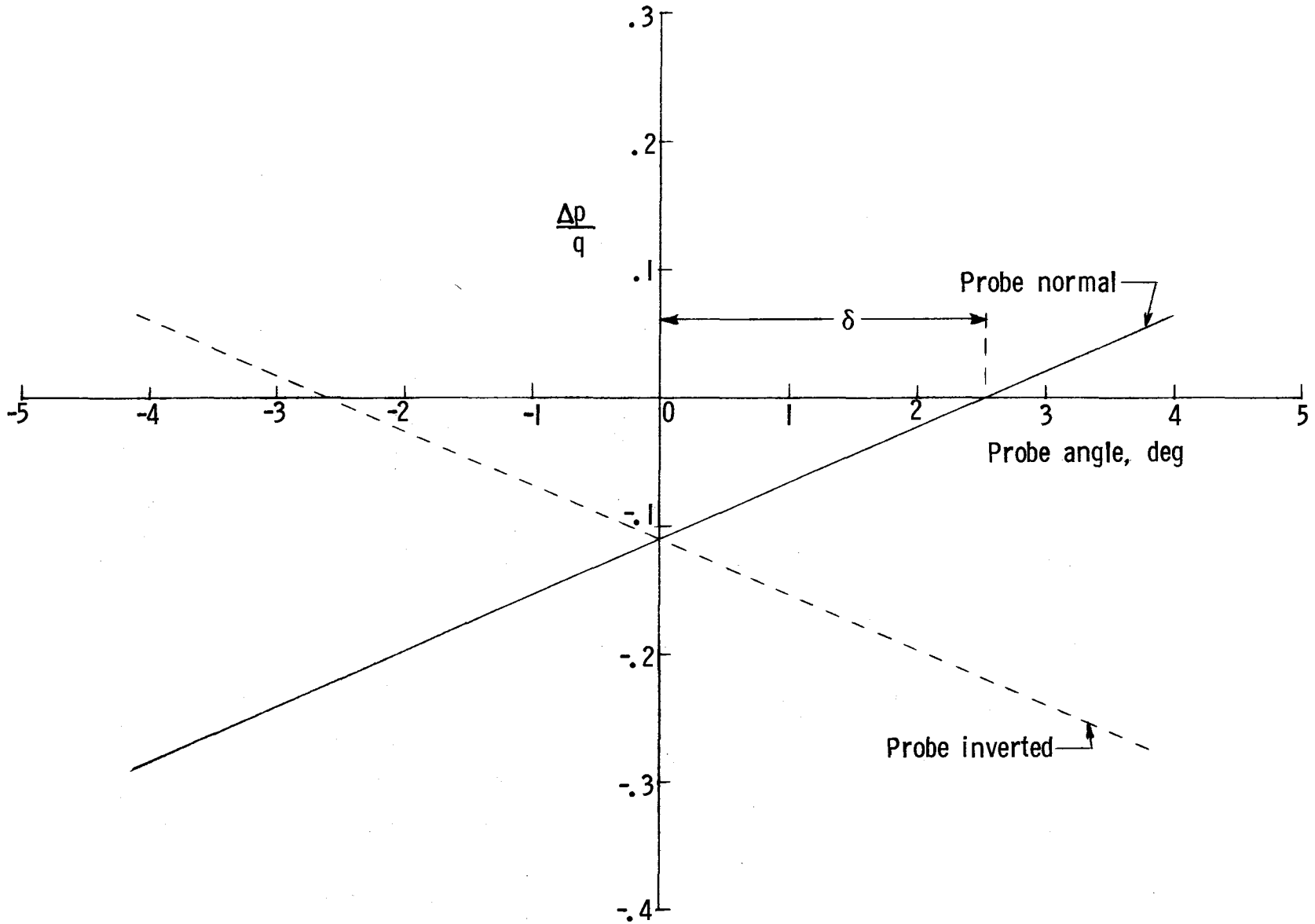

Figure 26.- Typical yawmeter probe calibration. x = 36 in.; y = 0 in.; z = -7.4 in.

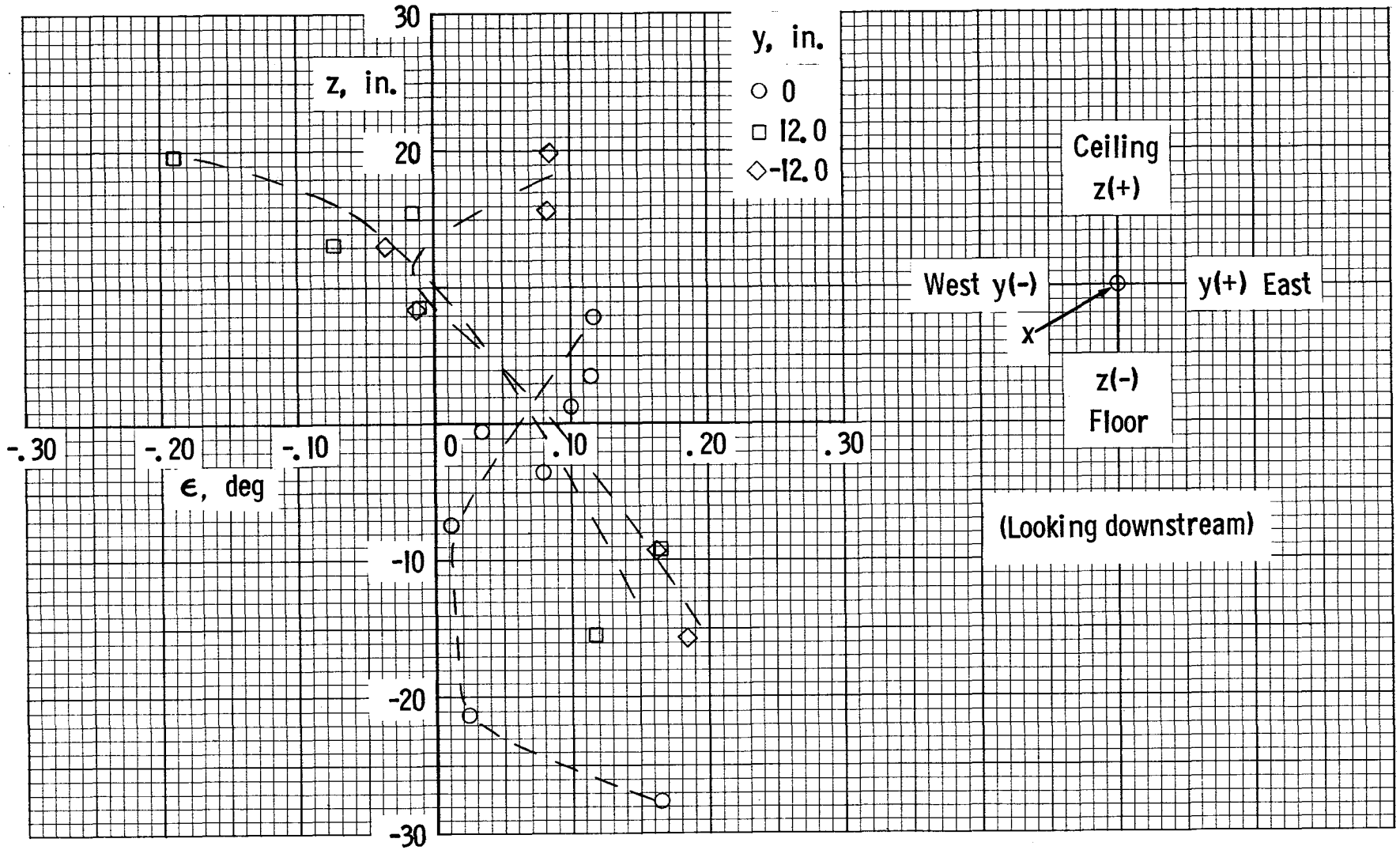

Figure 27.- Typical flow-angularity measurements in test section of tunnel.

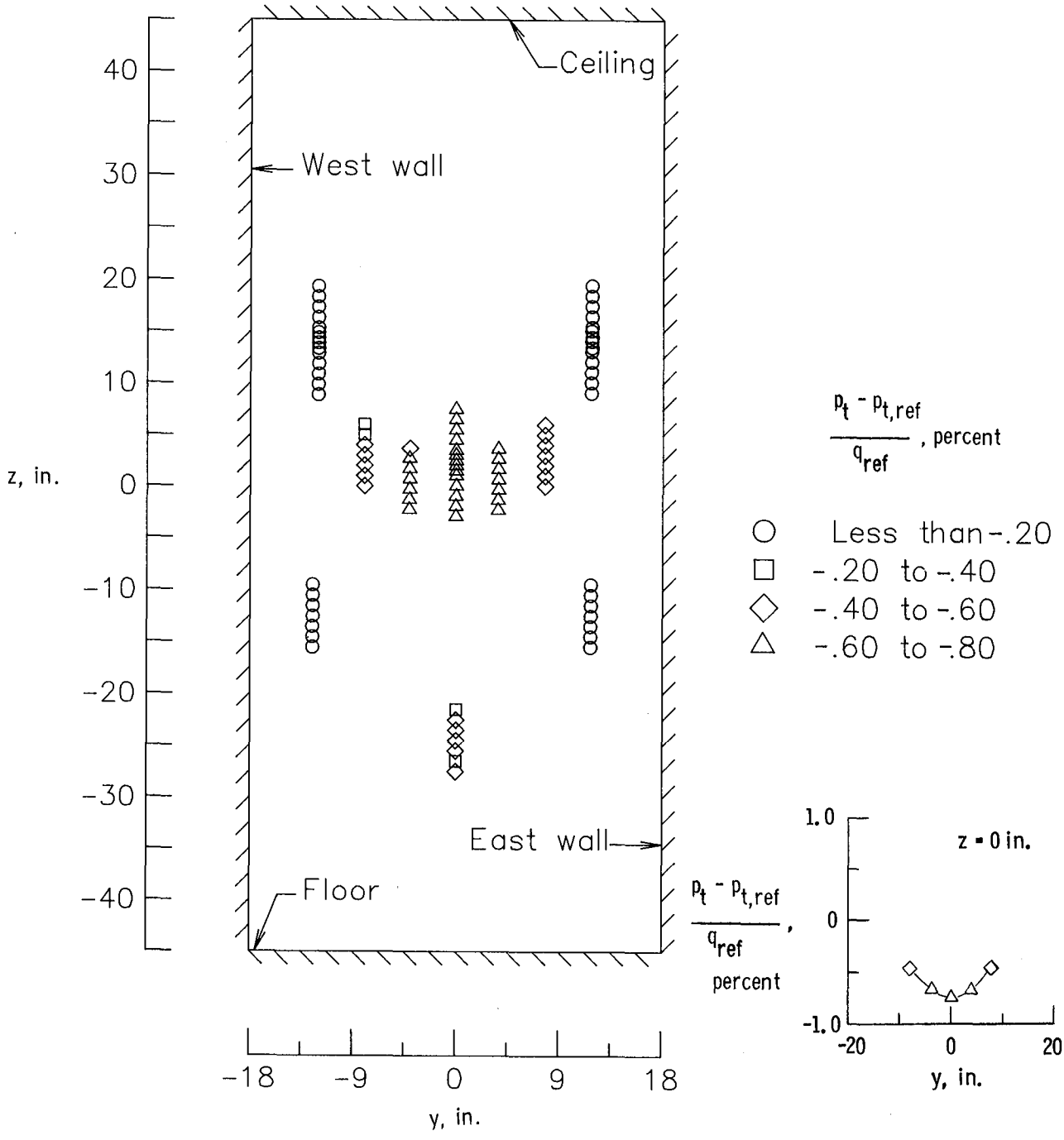

Figure 28.- Typical total-pressure surveys in test section of tunnel. x = 36 in.

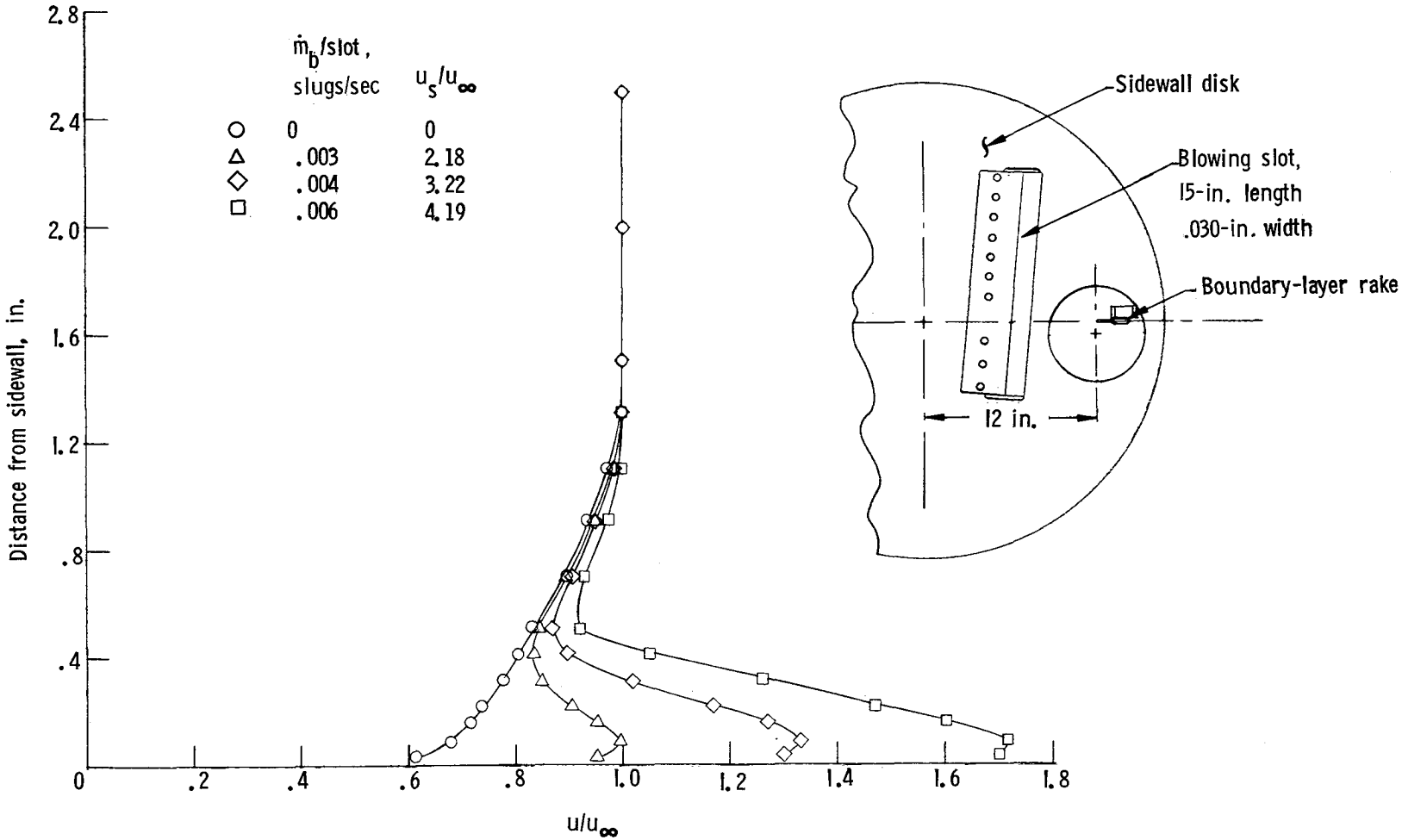

Figure 29.- Effect of tangential blowing (BLC) on boundary-layer velocity profiles on sidewall of test section. M = 0.22; R = 1.5 x 10^6 ft^{-1}; x = 12 in.

L-82-11,838

Figure 30.- Photograph of wake survey rake.

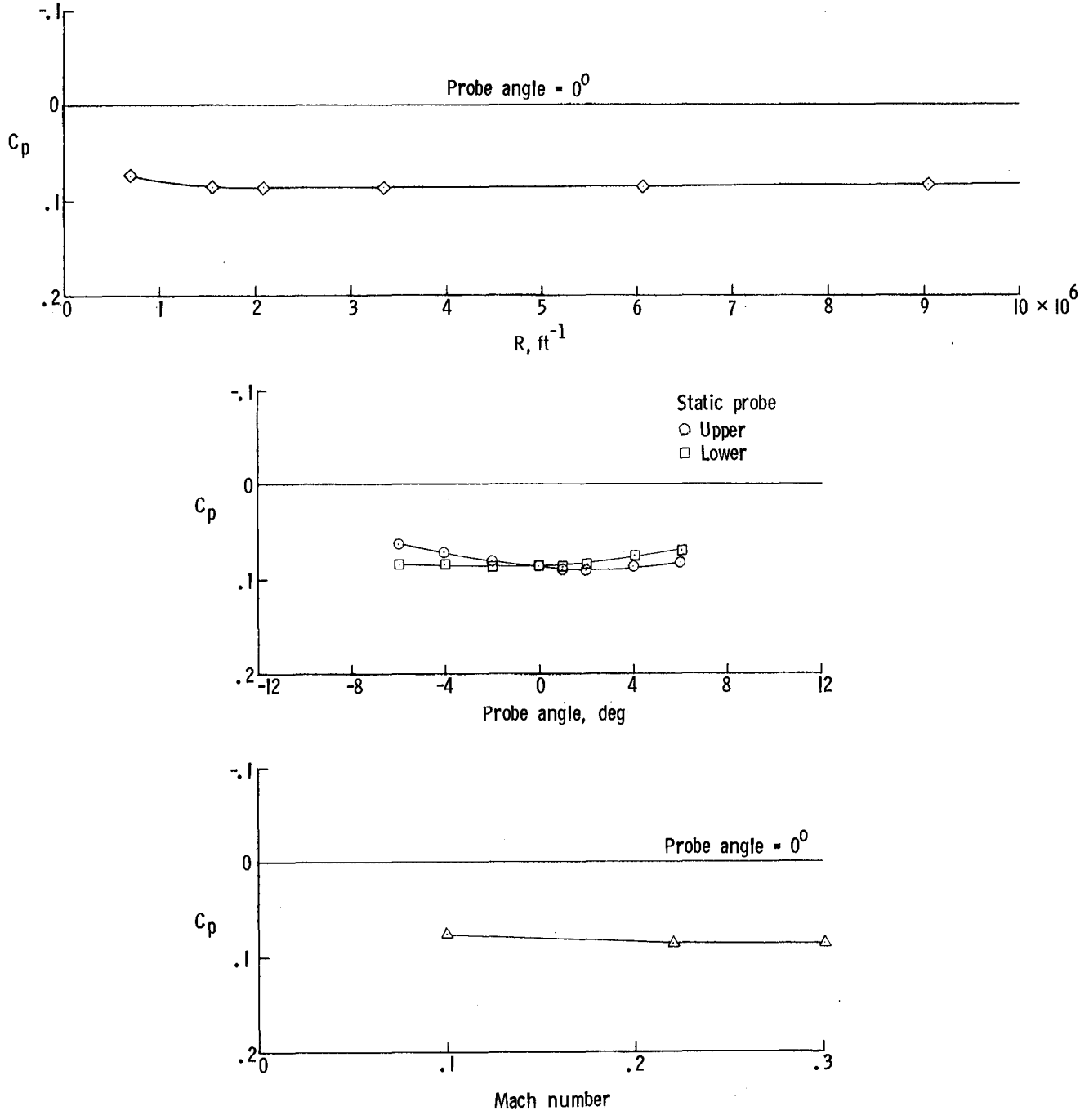

Figure 31.- Performance of standard static-pressure probe.

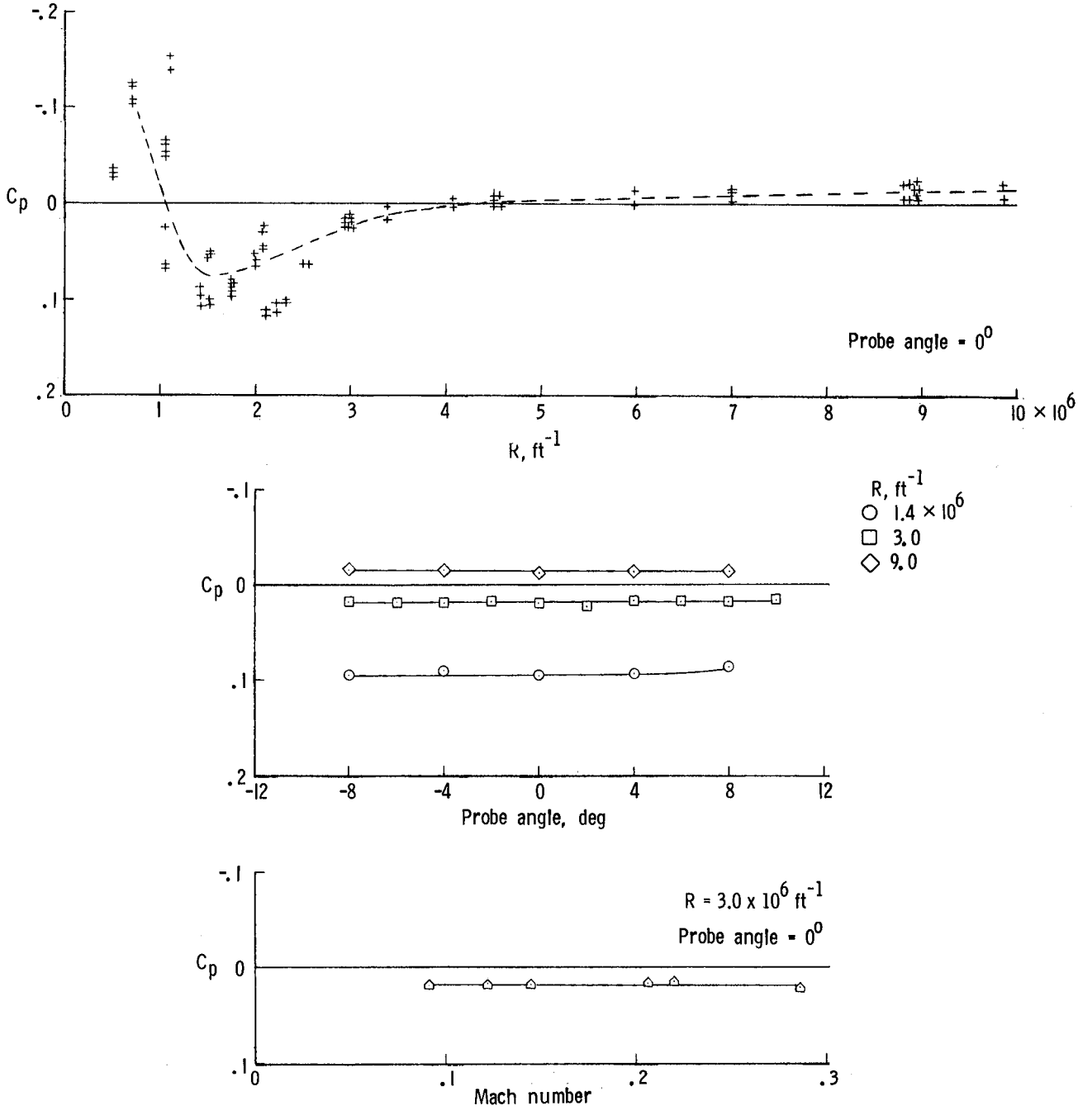

Figure 32.- Performance of disc static-pressure probe.

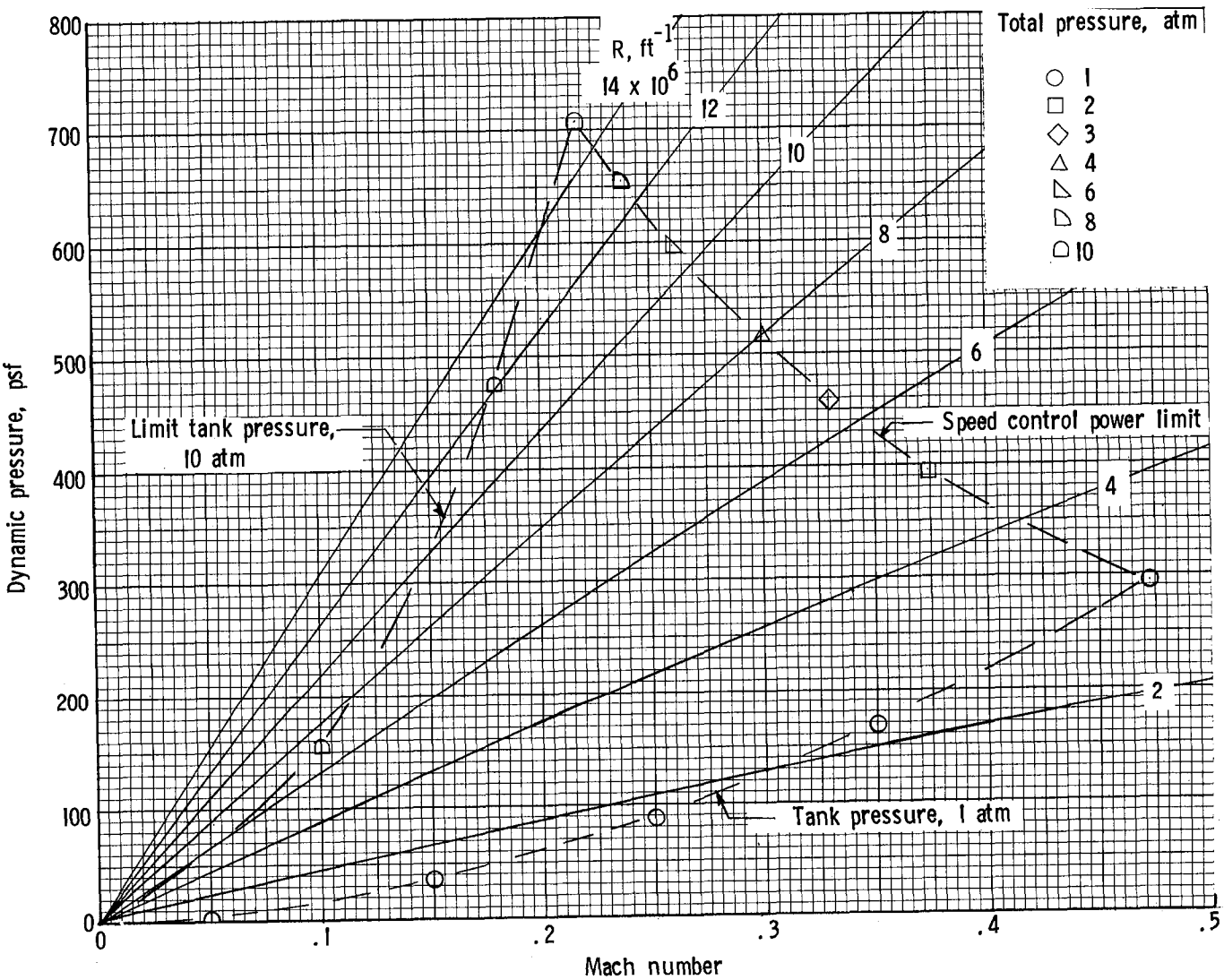

Figure 33.- Operational characteristics of Langley Low-Turbulence Pressure Tunnel.

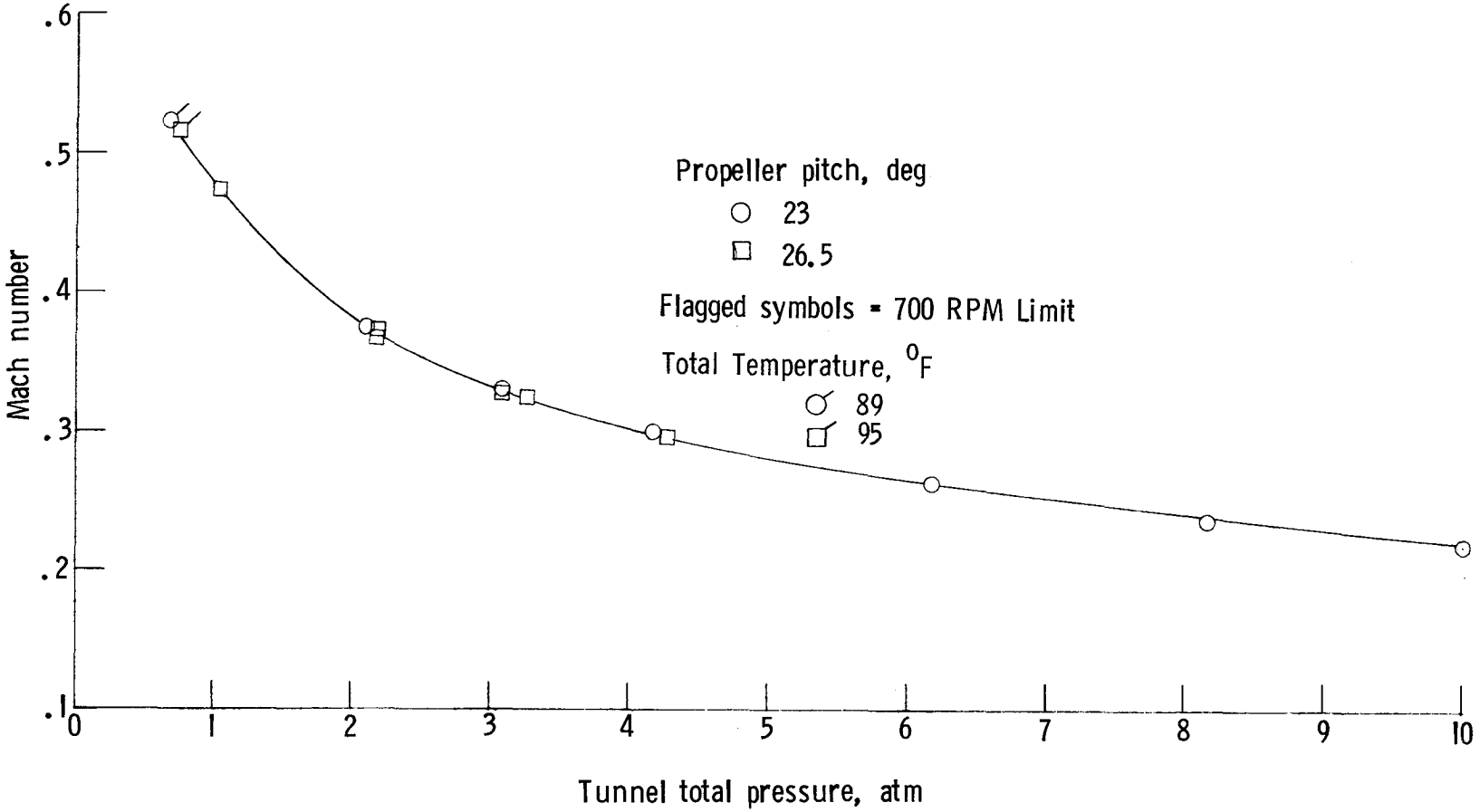

Figure 34.- Maximum Mach number capability of Langley Low-Turbulence Pressure Tunnel.

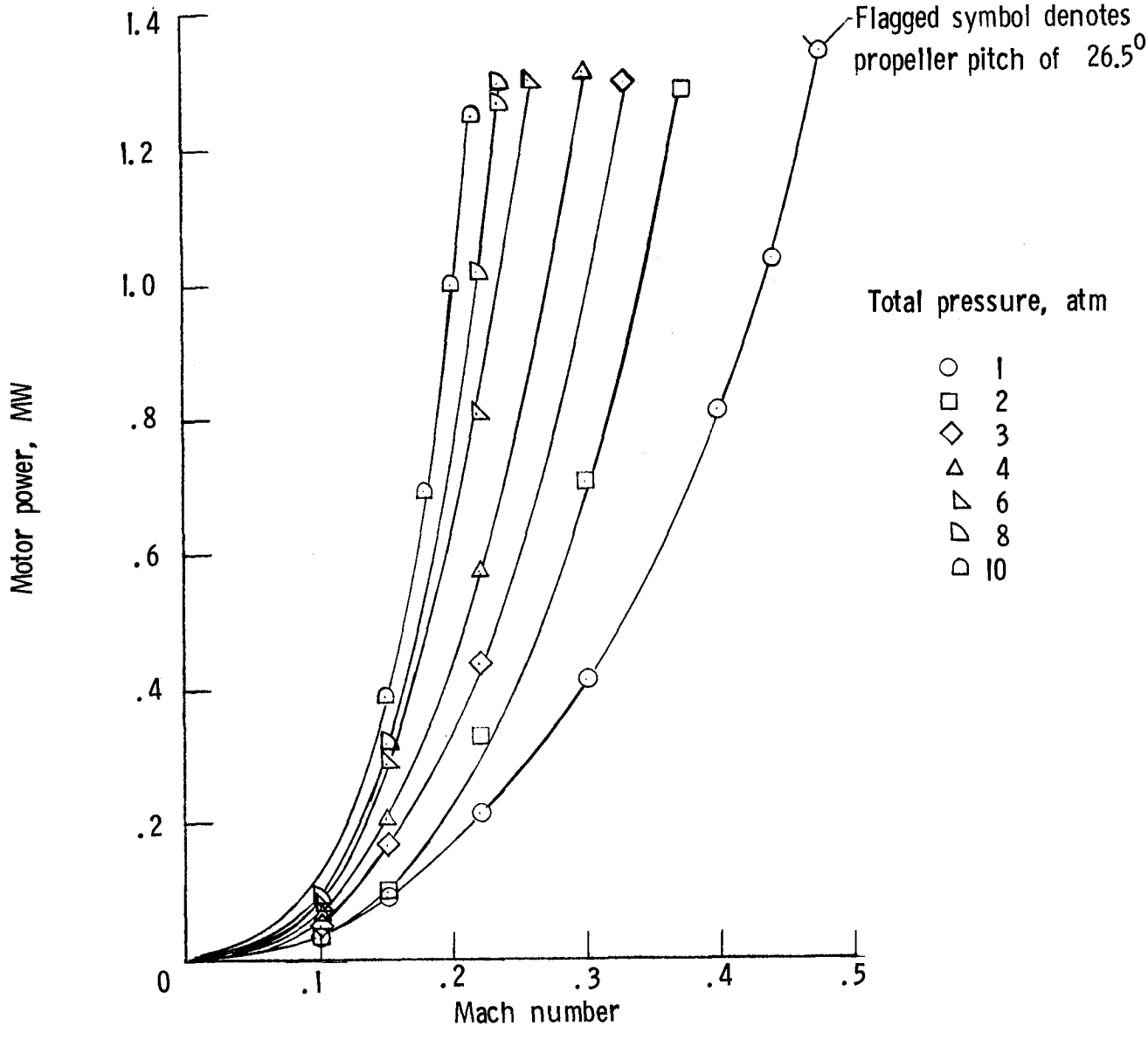

Figure 35.- Power requirements for main-drive motor for Langley Low-Turbulence Pressure Tunnel. Propeller pitch = 23°.

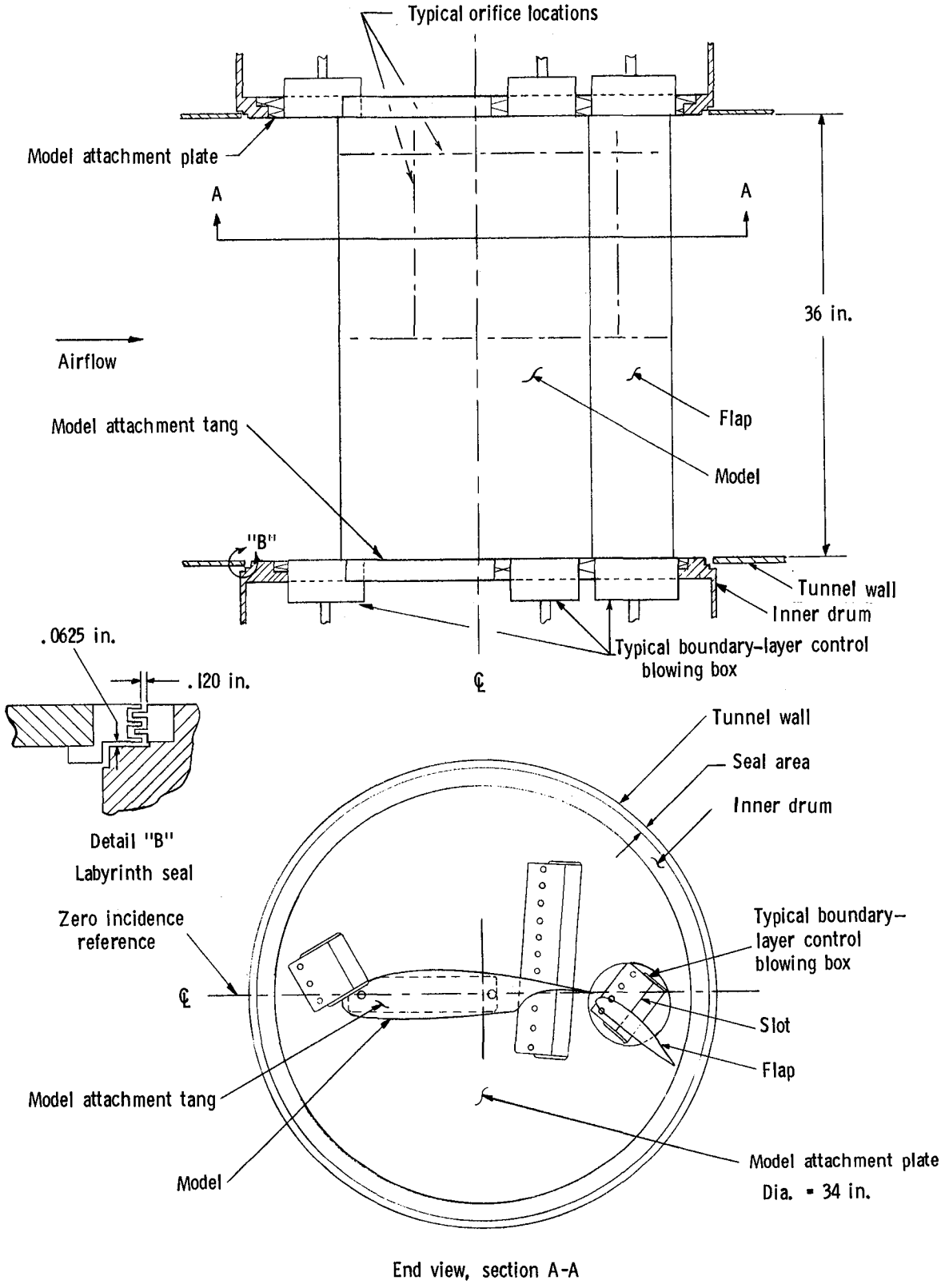

Figure 36.- NACA 4416 airfoil model with 35-percent-chord single-slotted flap mounted in wind tunnel.

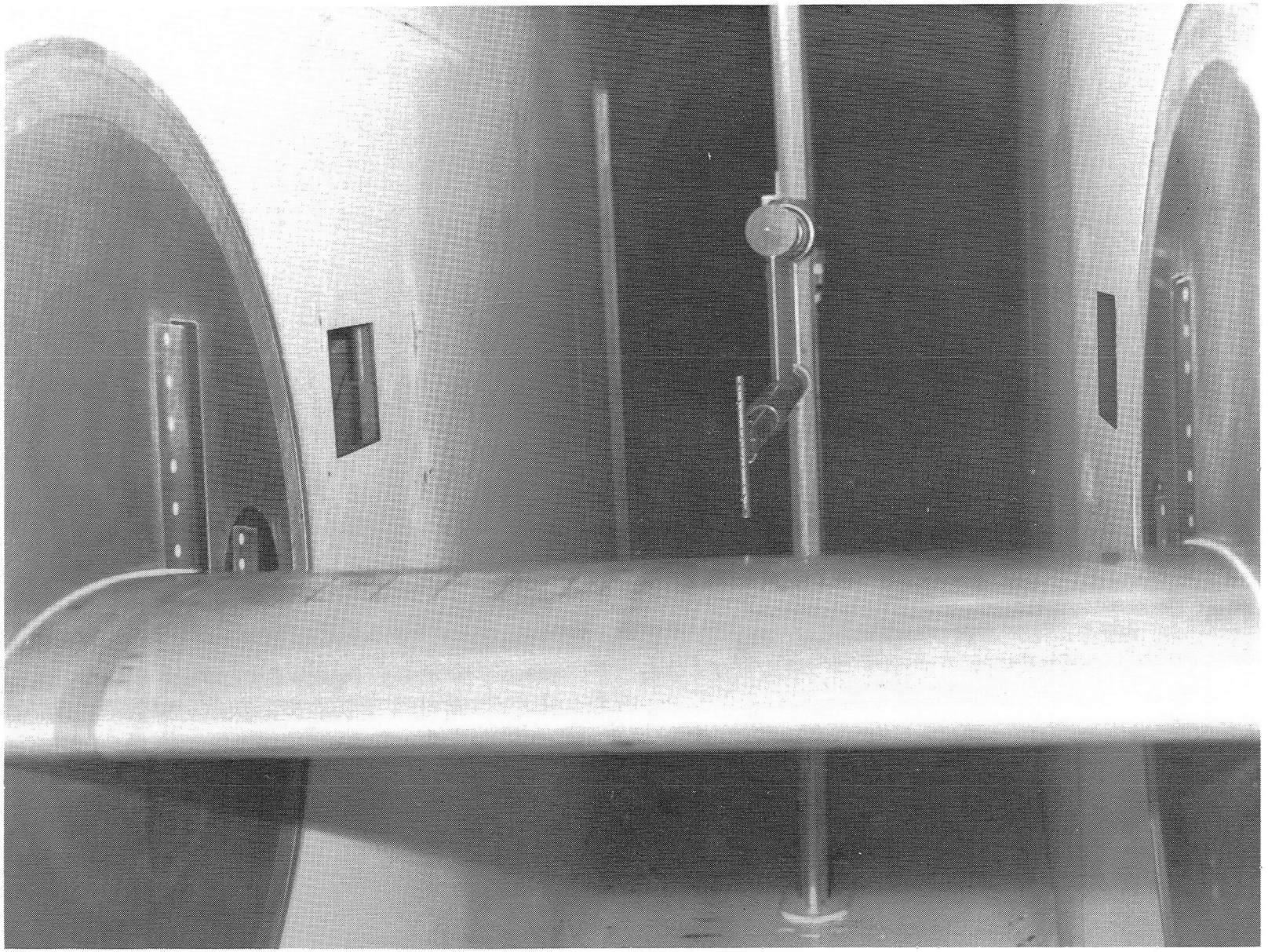

L-83-1135

Figure 37.- Photograph of NACA 4416 airfoil model mounted in wind tunnel.

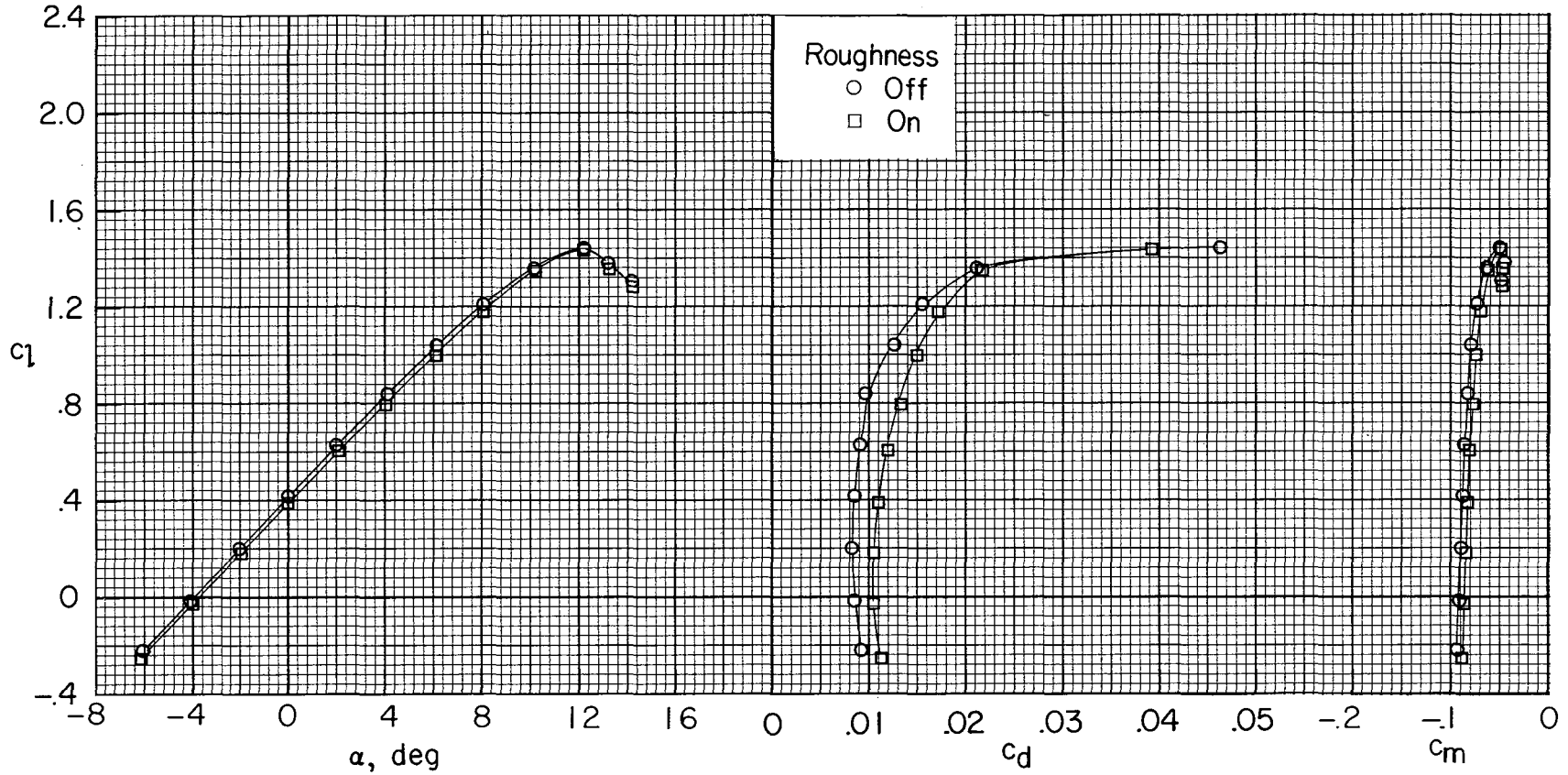

Figure 38.- Section characteristics for NACA 4416 airfoil with flap nested. M = 0.20; $R_c = 3.0 \times 10^6$; y/c = 0.0. Roughness size and location: upper surface - 0.0070-in. diameter, 0.06c; lower surface - 0.0083-in. diameter, 0.08c.

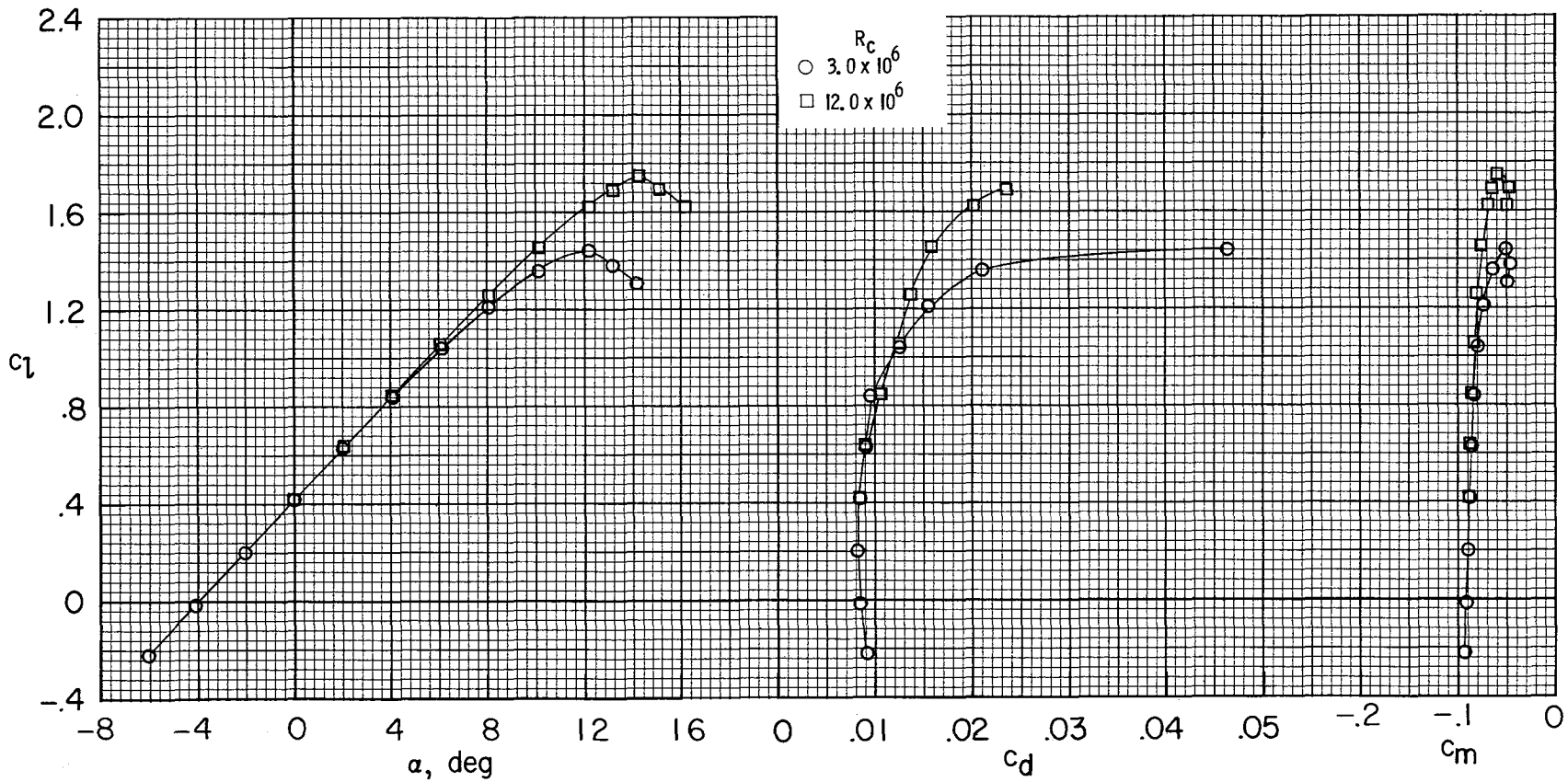

Figure 39.- Effect of Reynolds number on section characteristics for NACA 4416 airfoil with flap nested. Model smooth; M = 0.20; y/c = 0.0.

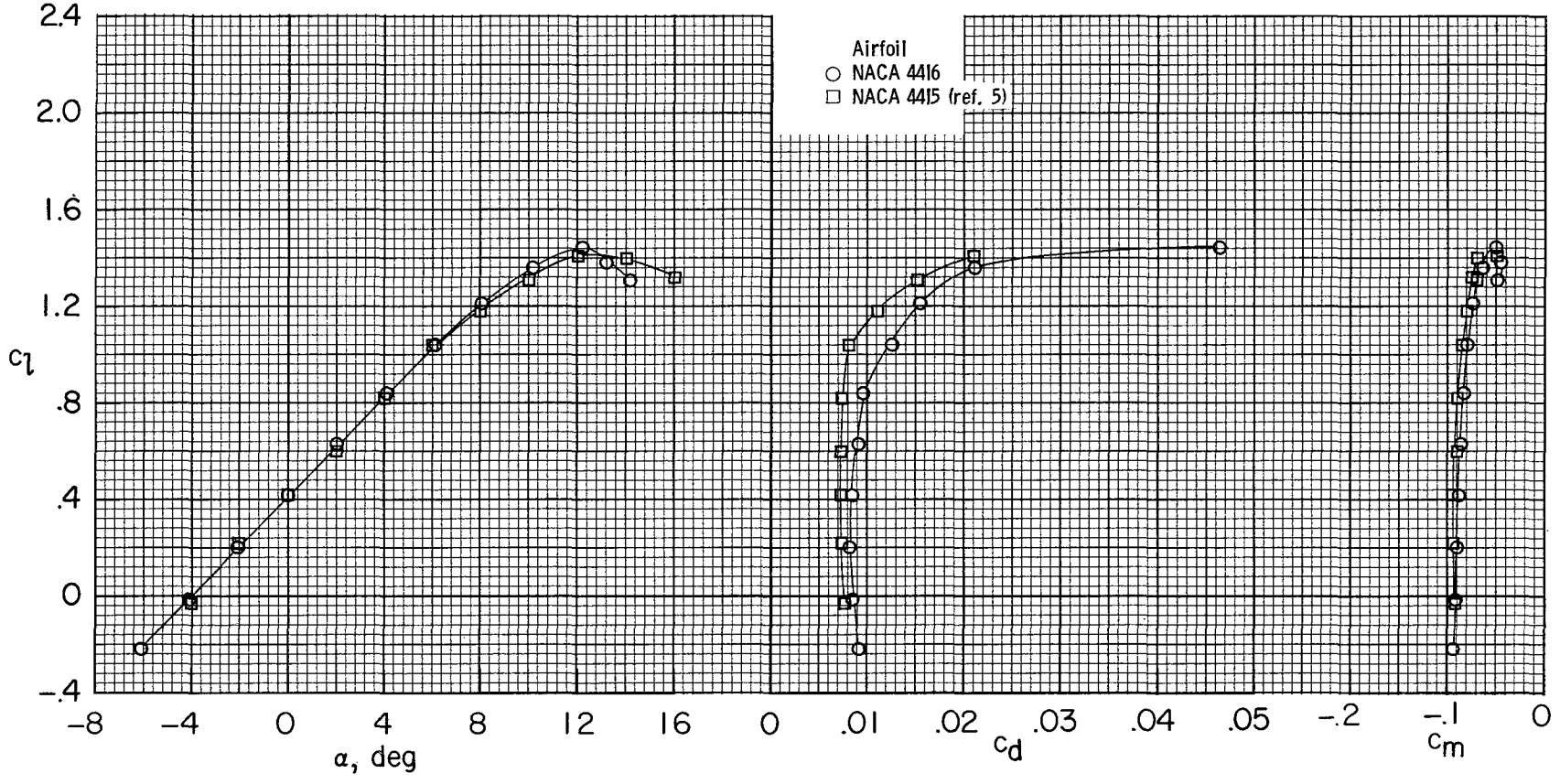

Figure 40.- Comparison of section characteristics for NACA 4416 (flap nested) and NACA 4415 airfoils. Models smooth; $M = 0.20$; $R_c = 3.0 \times 10^6$; $y/c = 0.0$.

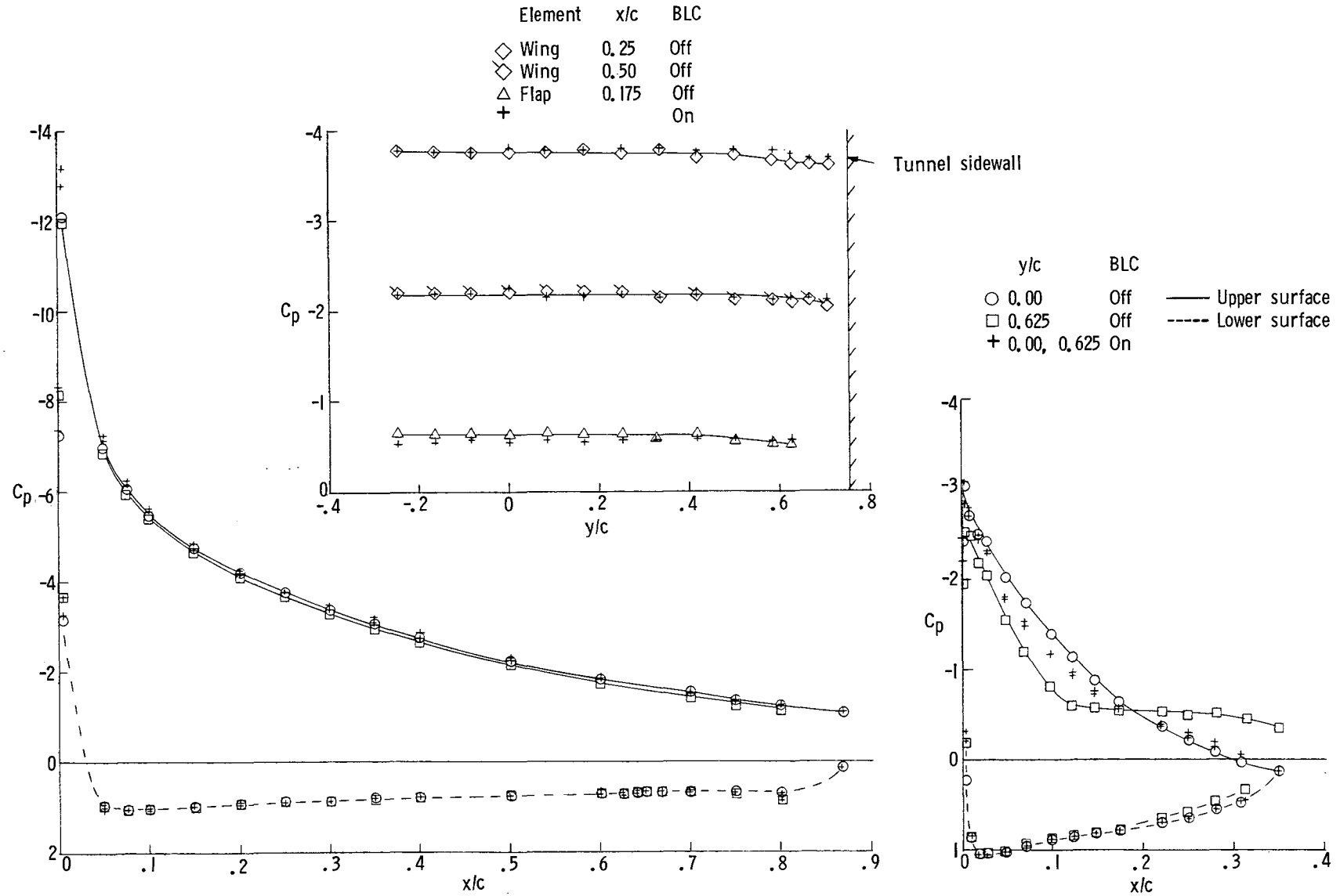

Figure 41.- Effect of sidewall boundary-layer control (BLC) on pressure data for NACA 4416 airfoil with flap deflected 30°. Roughness on; M = 0.20; $R_c = 3.0 \times 10^6$; $\alpha = 12°$. (x denotes airfoil abscissa.)

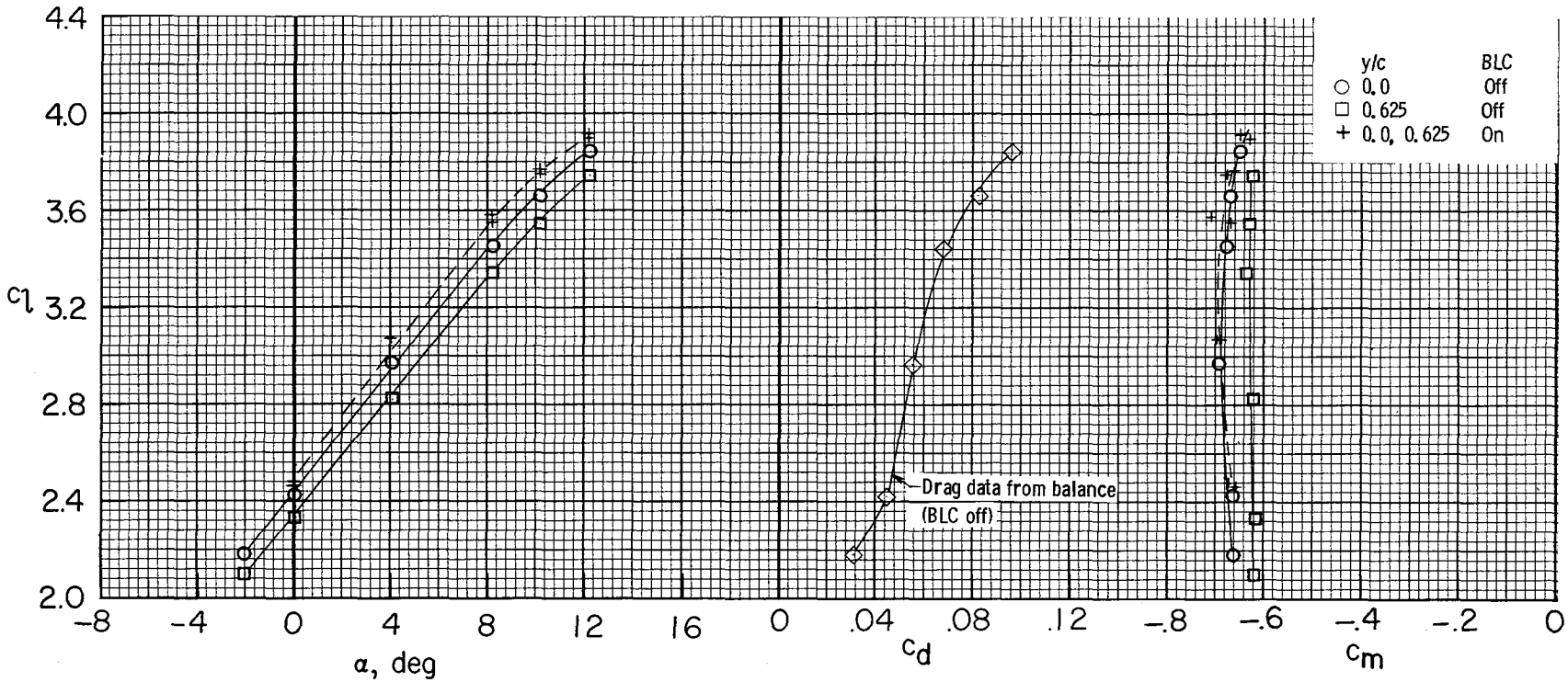

Figure 42.- Effect of sidewall boundary-layer control (BLC) on section characteristics for NACA 4416 airfoil with flap deflected 30°. Roughness on; M = 0.20; $R_c = 3.0 \times 10^6$.

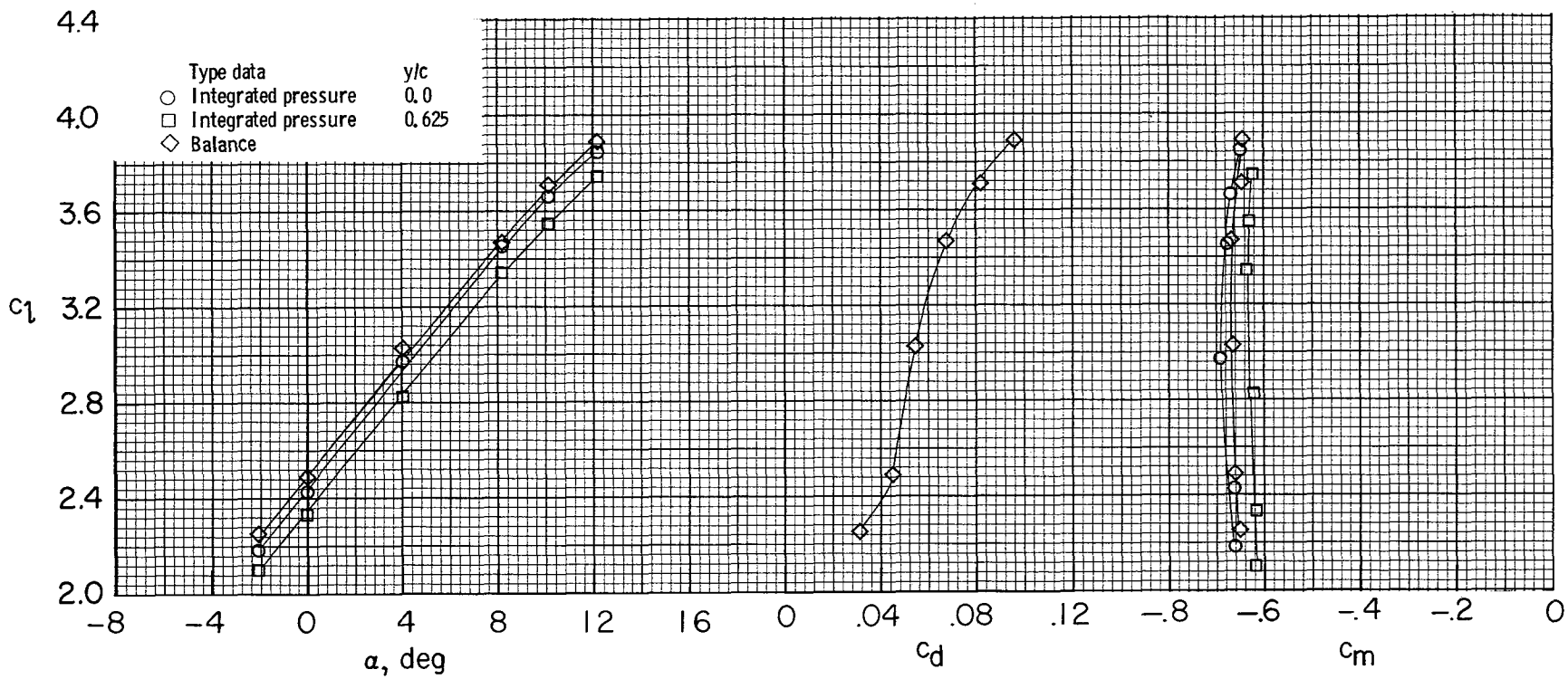

Figure 43.- Comparison of integrated pressure data and balance data for NACA 4416 airfoil with flap deflected 30°. Roughness on; M = 0.20; $R_c = 3.0 \times 10^6$; BLC off.

1. Report No.	2. Government Accession No.	3. Recipient's Catalog No.
NASA TP-2328		

4. Title and Subtitle	5. Report Date
RECENT MODIFICATIONS AND CALIBRATION OF THE LANGLEY LOW-TURBULENCE PRESSURE TUNNEL	July 1984
	6. Performing Organization Code 505-31-23-06

7. Author(s)	8. Performing Organization Report No.
Robert J. McGhee, William D. Beasley, and Jean M. Foster	L-15728
	10. Work Unit No.

9. Performing Organization Name and Address	11. Contract or Grant No.
NASA Langley Research Center Hampton, VA 23665	

12. Sponsoring Agency Name and Address	13. Type of Report and Period Covered
National Aeronautics and Space Administration Washington, DC 20546	Technical Paper
	14. Sponsoring Agency Code

15. Supplementary Notes

16. Abstract

A description is presented of recent modifications to the Langley Low-Turbulence Pressure Tunnel, and a calibration of the mean flow parameters in the test section is provided. Also included are the operational capability of the tunnel and typical test results for both single-element and multi-element airfoils. Modifications to the facility consisted of the following: replacement of the original cooling coils and antiturbulence screens and addition of a tunnel-shell heating system, a two-dimensional model-support and force-balance system, a sidewall boundary-layer control system, a remote-controlled survey apparatus, and a new data-acquisition system. A calibration of the mean flow parameters in the test section was conducted over the complete operational range of the tunnel. The calibration included dynamic-pressure measurements, Mach number distributions, flow-angularity measurements, boundary-layer characteristics, and total-pressure profiles. In addition, test-section turbulence measurements made after the tunnel modifications have been included with these calibration data to show a comparison of existing turbulence levels with data obtained for the facility in 1941 with the original screen installation.

17. Key Words (Suggested by Author(s))	18. Distribution Statement
Low-turbulence wind tunnel Low-speed wind tunnel Wind-tunnel calibration Wind-tunnel description	Unclassified - Unlimited Subject Category 02

19. Security Classif. (of this report)	20. Security Classif. (of this page)	21. No. of Pages	22. Price
Unclassified	Unclassified	63	A04

For sale by the National Technical Information Service, Springfield, Virginia 22161 NASA-Langley, 1984

National Aeronautics and Space Administration

Washington, D.C. 20546

Official Business
Penalty for Private Use, $300

THIRD-CLASS BULK RATE

Postage and Fees Paid
National Aeronautics and Space Administration
NASA-451

U.S.MAIL

NASA

DO NOT REMOVE SLIP FROM MATERIAL

Delete your name from this slip when returning material to the library.

NAME	MS
[illegible]	114
[illegible]	267
[illegible] Read Bldg 1297H Rm117	160
[illegible] Library	185
[illegible]	[illegible]
[illegible] 2/15/95	267
[illegible] 3/11/95	408A
V. ERIC ROBACK	408A

NASA Langley (Rev. May 1988)

RIAD N-75